Denise Aniceto Carreira

# Radioactive labeling of NP with albumin to study the biodistribution


2014

O que é bonito neste mundo, e anima,

É ver que na vindima

De cada sonho

Fica a cepa a sonhar outra aventura…

*Poema "Começo", Miguel Torga*

# Acknowledgements

Foremost, I would like to express my sincere gratitude to my advisors Professor Maria Filomena Botelho and Professor António Ribeiro, whose expertise, understanding, and patience, added considerably to my graduate experience. They supported me throughout my thesis with their vast knowledge whilst allowing me have autonomy.

I would like to express my deepest gratitude to Ana Margarida Abrantes for the continuous support of my master study and research, for her patience, motivation, enthusiasm, and immense knowledge. Her guidance helped me in all the time of research and writing of this thesis.

Marlene Lopes was always willing to help with *in vivo* studies and give her best suggestions. She helps me to develop my knowhow in pharmaceutical technology and was permanently allowing me a support in critical moments. For these reasons, not only, I would like to phrase my most profound thanks.

I would like to thank to radiopharmacists of Centro Hospitalar da Universidade de Coimbra and to nuclear medicine technologists of Instituto Português de Oncologia de Coimbra for exempt techenetium-99m provided for my research work.

I thank my fellow labmates in Biophysics Department: Ana Ferreira, Ana Moço, Ana Ribeiro, Gonçalo Brites, João da Encarnação, Kathleen Santos, Tânia Costa, Telmo Gonçalves, Tiago Sales, Ricardo Teixo and Sara Guerra for an excellent atmosphere for doing research and for the fun time I had in Coimbra. I also like to thank to Ana Brito, Catarina Mamede, Salomé Pires and Mafalda Laranjo for the kindness and encouraging words. I am also thankful to Fábio Gonçalves and Tiago Puga, nuclear medicine trainees, for the stimulating discussions and their participation in the *in vivo* studies.

A very special thanks goes out to Patrícia Carreira without her motivation, encouragement, understanding, parent-like support, generous care and the home feeling whenever I was in need during my master degree. I also wish thank to Ana Camara, João Jorge, Liliana Sousa and Ana Clarice Rodrigues for cheering me up and standing by me in bad and good times. Also I thank my friends in Faculty of Pharmacy, Ana Pica-milho and Tânia

Baptista, for the sleepless nights we were working together before deadlines, and for all the fun we have had in the last year.

*Por último, mas não menos importante, eu quero agradecer à minha família, os meus pais, a minha irmã e a minha afilhada, por todo o apoio que me têm dado ao longo da minha vida. Só com o seu incentivo, dedicação e coragem é que foi possível concluir este mestrado.*

# Index

# List of figures

# List of tables

# Abstract

Diabetes *mellitus* is characterized by hyperglycemia and there are three main types: type I, type II and gestational. The prevalence of diabetes is increasing and all patients with type I diabetes, and about 35% of type II diabetics require insulin therapy. When insulin is administrated by subcutaneous injection, every tissue are exposed to the same concentration and only a fraction of the injected dose is delivered to the liver. NP (NP) have been considered for oral insulin delivery by stabilizing and ensuring its biological activity *in vivo* and by facilitating intestinal delivery and absorption. Thus, the insulin delivered by the NP mimic the endogenous insulin. The aim of this work was study the biodistribution of the NP, therefore the biodistribution of $^{99m}$Tc-BSA(bovine serum albumin) and $^{99m}$Tc-BSA-NP was carried out after the BSA and BSA-NP radiolabeling and a quality control procedure was developed and optimized.

NP were formulated by emulsification/internal gelation, which nucleus consists of alginate, dextran sulfate, calcium carbonate and insulin following complexation with chitosan and coated with BSA. To optimize radiolabelling procedure of BSA, different parameters were tested, namely, ligand and reducing agent concentration, pH, radionuclide activity, temperature and incubation time. To optimize the quality control of the radiolabeling procedure different mobile phases and stationary phases was tested. To evaluate radiopharmaceuticals biodistribution, a comparative study between $^{99m}$Tc-BSA and $^{99m}$Tc-BSA-NP was developed. The complexes were administered by gavage in Balb/c mice. The animals were killed at different time intervals: 0, 30, 60, 90, 120, 180, 360 and 1440 minutes after administration. Gastrointestinal tract and several organs and fluids were collected. Furthermore, the gastrointestinal content was separated from the gastrointestinal wall, whose was cleaned. All biological material collected was weighed and its radioactivity was evaluated by image processing. The percent of administered activity *per* milligram of organ was calculated.

Radiochemical purity was determined by two systems with strips of instant thin-layer chromatography-silica gel (ITLC-SG) as stationary phase and NaCl (sodium chlorate) and ACD (acid citrate-dextrose) as mobile phases. The radiochemical purity obtained was higher than 95% and remain stable at least for 6h. These results were obtained by using: sodium thiosulfate 10mg.ml$^{-1}$; HCl (hydrochloric acid), N; BSA 10mg.ml$^{-1}$; phosphate buffer (pH 7.4) (1.0/1.0/2.5/2.0) (v/v/v/v) and 1110 to 2220 MBq of $Na^{99m}TcO_4^-$ (sodium perthecnetate). The biodistribution studies revealed that $^{99m}$Tc-BSA-NP have different profiles of adhesion to the stomach and small intestine epithelium regardless of the profile of the contents' progression

in the gut, comparatively to the $^{99m}$Tc-BSA biodistribution. Six hours after administration most of the complex was in the large intestine and all the activity was eliminated 24h after administration.

The labelling procedure of BSA was stable, reproducible and reveals potential to track albumin. Differences between $^{99m}$Tc-BSA-NP and $^{99m}$Tc-BSA seem to do due to the mucoadhesive properties of the NP' polymers, namely chitosan. However, to evaluate insulin absorption future studies should be carried out.

# Resumo

A diabetes *mellitus* é caracterizada por hiperglicemia e a doença manifesta-se em diferentes tipos, sendo os principais, o tipo 1, o tipo 2 e a gestacional. A prevalência da diabetes tem aumentado e todos os doentes com diabetes tipo 1 e cerca de 35% dos diabéticos tipo 2 têm de recorrer à terapia com insulina. A insulina administrada pela via subcutânea leva a uma exposição de todos os tecidos à mesma concentração da insulina e apenas uma fracção da dose injectada é captada pelo fígado. As nanopartículas (NP) para administração oral da insulina têm vindo a ser consideradas por assegurarem e estabilizarem a sua actividade biológica *in vivo*, mas também por facilitarem a sua entrega e absorção em meio intestinal. Desta forma, a insulina administrada com recurso às nanopartículas mimetizaria a insulina endógena.

O objectivo deste trabalho era estudar a biodistribuição das nanoparticulas, para tal procedeu-se ao estudo da biodistribuição do $^{99m}$Tc-BSA(bovine serum albumin) e do $^{99m}$Tc-BSA-NP, após o desenvolvimento e optimização do controlo de qualidade e da marcação radioactiva do BSA e do BSA-NP.

As nanopartículas foram produzidas por emulsificação/gelação interna, o seu núcleo é constituído por alginato, sulfato de dextran, carbonato de cálcio e insulina, sofre complexação com o quitosano e é revestido por BSA. Relativamente à optimização do controlo de qualidade do procedimento de radiomarcação foram testadas diferentes fases móveis e fases estacionárias. Para optimizar a radiomarcação do BSA foram testados diferentes parâmetros, nomeadamente, a concentração de ligando e agente redutor, pH, a actividade do radionuclídeo, temperatura e tempo de incubação. Para avaliar a biodistribuição dos radiofármacos foi realizado um estudo comparativo entre o $^{99m}$Tc-BSA e o $^{99m}$Tc-BSA-NP. Ambos os complexos foram administrados por gavagem a ratinhos *Balb/c*. Os animais foram sacrificados a diferentes intervalos de tempo: 0, 30, 60, 90, 120, 180, 360 e 1440 minutos após a administração. O tracto gastrointestinal e vários órgãos e fluidos foram recolhidos, para além disso, o conteúdo gastrointestinal foi separado da parede gastrointestinal, que por sua vez foi lavada. Todo o material biológico recolhido foi pesado e a radioactividade foi avaliada pelo processamento das imagens e foi calculada a percentagem de actividade administrada por miligrama.

A pureza radioquímica foi determinada com recurso a dois sistemas cromatográficos, cuja fase estacionária eram tiras de cromatografia em camada fina instantânea-gel de sílica (do inglês, ITLC-SG) e a fase móvel era NaCl (cloreto de sódio) e ACD (ácido de citrato-dextrose). A pureza radioquímica obtida foi superior a 95% e mantem-se estável por 6h.

Estes resultados foram obtidos com 10mg.ml$^{-1}$ de tiossulfato de sódio; HCl (ácido clorídrico), N; 10mg.ml$^{-1}$ de BSA; tampão fosfato a pH 7.4, (1.0/1.0/2.5/2.0) (v/v/v/v) e 1110 to 2220 MBq de $Na^{99m}TcO_4^-$ (pertecnetato de sódio). Os estudos de biodistribuição revelaram que o $^{99m}$Tc-BSA-NP tem um perfil diferente de adesão à parede do estomago e do intestino delgado, independente do perfil de progressão do conteúdo ao longo do tracto gastrointestinal, quando comparado com a biodistribuição do $^{99m}$Tc-BSA. Seis horas após a administração dos radiofármacos estes encontram-se maioritariamente no intestino grosso e 24h após a administração toda a actividade já foi eliminada.

O procedimento de marcação do BSA é estável e reprodutível e revela potencial para acompanhar o BSA. As diferenças entre o $^{99m}$Tc-BSA-NP e o $^{99m}$Tc-BSA parecem ser devidas às propriedades mucoadesivas dos polímeros que constituem as nanoparticulas, mais concretamente o quitosano. Contudo, para avaliar a absorção da insulina devem ser efectuados outros estudos.

# List of abbreviations and acronyms

% - Percent

µg - Micrograms

µL - Microliter

µm - Micrometer

µM - Micromolar

$^{111}$In - Indium-111

$^{11}$C - Carbone-11

$^{123}$I - Iodine-123

$^{18}$F - Fluor-18

$^{201}$Tl - Talium-201

$^{67}$Ga - Galium-67

$^{68}$Ga - Galium-68

$^{99}$Mo - Molybdenium-99

$^{99m}$Tc - Technetium-99m

$^{99m}TcO_4^-$ - Pertechnetate

$^{99m}$Tc-RH - $^{99m}$Tc-reduced-hydrolyzed

$^{99}$Tc – Technetium-99

ACD - Acid citrate-dextrose

Al - Aluminum

Ba - Barium

BSA - Bovine serum albumin

dL - Deciliter

DNA - Deoxyribonucleic acid

e.g. - E*xemple gratia*

FDG - Fluorodeoxyglucose

Fe - Iron

Fig. - Figure

FITC - Fluorescein isothiocyanate

*g* - *g* force

G - α-L-guluronic

$H_2O$ - Water

HCl - Hydrochloride acid

HDP - Hydroxymethylenediphosphonic acid

HIV - Human Immunodeficiency Virus

HSA - Human Serum Albumin

ITLC - Instant thin-layer chromatography

IU - International unit

kDa - KiloDalton

keV - Kiloelectron-Volt

KHz - Kilohertz

L –Liter

M - β-D-mannuronic acid

m – Mass

v - Volume

MBq - Mega bequerel

MDP - Methylene diphophonate

Mg - Magnesium

mg - Milligram

min - Minutes

mmol - Milimolar

mV - MiliVolts

N - Nitrogen

Na(Tl) - Sodium iodide with thallium doping

$Na^{99m}TcO_4^-$ - Sodium pertechnetate

nm - Nanometer

No. - Number

NP - NP

O - Oxygen

O/W - Oil in water

$OH^-$ - Hydroxide

P - Phosphorus

PACA - Poly(alkylcyanoacrylate)

PET - Positron Emission Tomography

pHSA - Plasma-derived HSA

PIBCA - Polyisobutylcyanoacrylate

$pK_a$ - Acidity constant

PLA - Polylactic acid

PLGA - Poly(lactic-co-glycolic acid)

PMMA - Poly(methylmethacrylate)

PMT - Photomultiplier Tubes

$R_f$ - Retention Value

RNAm - Messenger Ribonucleic Acid

ROIs - Regions of interest

S - Sulfur

SA - Polysilicic Acid

SD - Standard deviation

SG - Silica Gel

-SH - Sulfhydryl group

Sn – Stannous

SPECT – Photon Emission Computed Tomography

Sr - Strotium

$t_{1/2}$ - Half-life

Tc - Technetium

W/O - Water in oil

# 1. Introduction

## 1.1 Diabetes *mellitus*

Diabetes *mellitus* is a descriptive term for a family of disorders that are characterized by chronic carbohydrate intolerance and the development of long-term medical complications. Under normal circumstances, the body must maintain blood glucose concentrations ranging 60-109 mg/dL (3.3-6.1 mmol/L) during fasting to avoid hypoglycemia and hyperglycemia. When hyperglycemia is persistent, diabetes *mellitus* is diagnosed (KNOWLER, 2005). The number of diabetic patients has been sharply increasing around the world, assuming an epidemic dimension. It is predicted that in 2030 366.2 million of people will have diabetes *mellitus* (WILD, *et. al.*, 2004).

Blood glucose concentrations are controlled primarily by hormones that regulate the rates of glucose consumption. The primary hormonal regulators of glucose production and consumption are insulin and glucagon, both produced by pancreas. Insulin release is stimulated by the increasing of blood glucose and also by the increasing of amino acid concentration after meals. In order to act on target tissues, insulin must bind to the insulin receptor, present on many types of cells, although the major sites of its location are the liver, muscle and adipose tissue. The balance between insulin secretion and glucagon secretion maintains the blood glucose concentration within strict limits. When insulin concentrations fall, glucagon concentrations rise, accounting for hyperglucagonemia, which is characteristic of diabetic states (KNOWLER, 2005).

Generally, diabetes *mellitus* is characterized by high blood glucose levels and the chronic states of disease have several complications, such as diabetic retinopathy with vision loss, nephropathy, peripheral neuropathy, and other several dysfunctions such as at gastric, intestinal, genito-urinary and sexual level. Furthermore, diabetes increases the prevalence of cardiovascular atherosclerosis, peripheral vascular and cerebrovascular disease (GEISS, 2000; KNOWLER, 2005).

There are different types of diabetes, such as type I, type II, gestational and other types. Type I diabetes is characterized by pancreatic $\beta$ cell destruction leading to absolute insulin deficiency, and it can be immune-mediated or idiopathic. Generally it begins in the childhood or in the adolescence, although it can occur in any age and represents 5% to 10% of the cases of diabetes. This diabetic type is characterized by total absence of insulin production and for this reason the need of insulin therapy is imperative (GEISS, 2000).

Type II diabetes is the most common, representing 90% of the diabetic patients and it is characterized by metabolic states that range from predominantly insulin resistance with relative insulin deficiency to a predominantly secretory defect with insulin resistance without a relation to autoimmune mechanisms. In these cases the origin of disease is related to

environmental and genetic factors. The therapy includes antidiabetic drugs and the insulin therapy is just an alternative that represents 35% of the patients with type II (GEISS, 2000).

Gestational diabetes *mellitus* is diagnosed when hyperglycemia of any degree is first recognized during pregnancy. Thus, there is possibility that diabetes occurs before the pregnancy but remained unrecognized until its medical visits. The definition applies regardless the method used to control glycemia, diet or insulin, during pregnancy and even this disorder persists postnatal (GEISS, 2000).

Normally the other type appears due to genetic defects related to pancreatic β cells function, insulin action or exocrine pancreas function (e.g. pancreatitis, pancreatectomy, tumors, cystic fibrosis). It can also be related to endocrinopathy (e.g. acromegaly, glaucoma, pheochromocytoma, hyperthyroidism, somatostatinoma). Furthermore, diabetes can be induced by drugs (e.g. streptozotocin, alloxan and the rodenticide Vacor are likely to cause permanent diabetes) and infections (GEISS, 2000; GITTOES, *et. al.*, 2010).

### 1.1.1 Insulin

Insulin is an anabolic protein produced by the β cells of pancreatic islets of Langerhans, generated prions from insulin precursor composed by three polypeptide chains, A, B and C. The proinsulin precursor is cleaved and stored in Golgi secretory vesicles, where scission of C chain occurs and the final form of insulin is obtained (figure 1). The A chain has two α-helix ($A_1$-$A_8$ and $A_{13}$-$A_{21}$) linked to each other in an antiparallel way, while the B chain has a central α-helix ($B_9$-$B_{19}$), flanked by extended amino- and carboxyl-terminal strands. Some residues of the A chain form an apolar nucleus, being insulin surface composed by both polar and apolar residues. Thus, the hormone has a compact three-dimensional structure, consisting on three helices and three conserved disulfide bridges (figure 1). This structure is determined by disulfide bridges position and *Van der Waals* strength which are essential for insulin activity (CHIEN, 1996).

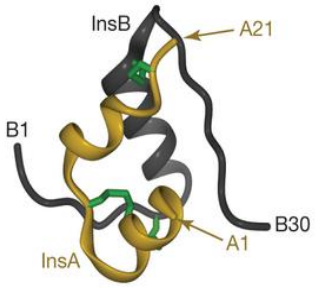


Figure 1 – Insulin structure. InsA represents A chain of insulin, InsB represent B chain of insulin and the disulfide bridges are represent in green. Extracted from MENTING 2012.

Insulin structure is sensible to high temperatures, high humidity, organic solvents, mechanical agitation, ultrasounds, and water-solvent and water-air interfaces. These factors can lead to molecular degradation, denaturation or insulin aggregation (BRANGE, 1987).

In physiological conditions the insulin concentration is lower than $10^{-3}$μM to ensure its biological activity. In higher concentration, insulin has tendency to dimerize and lose the monomeric form that is responsible for the hypoglycemic activity of insulin. Insulin molecule has fifty-one amino acids, six of them with positive charge and ten with negative charge. The isoelectric point of insulin is between 5.3 and 5.4 (BRANGE, 1987).

Insulin pharmacodynamics is complex and it is dependent of several factors, such as its administration pathway, hepatic function and glucose concentration. As previously mentioned, insulin regulates glucose metabolism, but it also is involved in lipogenesis, in decreasing of lipolysis and ketone production. Furthermore, insulin promotes DNA synthesis, cell's replication, and interacts with insulin-like growing factors and relaxins, influencing modulation of transcription and $RNA_m$ cell contents (CHIEN, 1996). In some tissues like muscles, insulin promotes glucose and amino acids uptake. In the liver, insulin stimulates glucose storage in the glycogen form, decreasing gluconeogenesis and increasing triglycerides production from glucose (CHIEN, 1996).

Liver and kidney are the principal pathways to insulin clearance. The first-pass extraction in the liver rounds 70% while the kidney metabolism degrades 10-40% of insulin per day. Insulin degradation occurs by catalysis of the reducing links of disulfide bridges by the insulin enzyme, insulinase. These reduced chains are then hydrolyzed in smaller fragments, which can occur in the liver, pancreas, muscle and adipose tissues (CHIEN, 1996).

### 1.1.2 Insulin therapy

The conventional insulin therapy consists in its subcutaneous administration being its bioavailability between 55 and 77% (GEISS, 2000). The most frequent complication of insulin therapy is hypoglycemia, besides the fact that when insulin is injected subcutaneously, it is exposed to all tissues in the same concentration and just a fraction of the injected dose is provided to the liver. Muscles and adipocytes can thus respond to the injected dose without hepatic processing of the insulin supply. Therefore, the excessive exposure of the vascular system and other smooth muscles to injected insulin may trigger its damaging overstimulation of growth, cell division and other metabolic responses that form the continuum of diabetic complications (REIS, *et. al.*, 2006; GEISS, 2000).

Newer methods of insulin delivery have been developed, including insulin pen systems, aerosol injectors, insulin inhalers, infusion pumps and jet injectors (AL-TABAKHA 2008).

Insulin pen systems (figure 2A) eliminate the inconvenience of carrying separately insulin, syringes and needles, moreover they are quick and easy to use, discreet, durable, flexible and do not need refrigeration. To use this device, the diabetics must attach a needle, prime the pen, set the dose by a dial and depress the plunger to administer subcutaneously the selected dose (AL-TABAKHA, 2008; SELAM, 2010). The insulin pump (figure 2B) permits a continuous subcutaneous insulin infusion that can be adjusted to the specific need of the patient in order to maintain the basal levels of insulin and glucose in the blood throughout the day. The pump device allows that the patient have an overall quality of life, however, if the insulin delivery is interrupted by infusion set malfunction, needle displacement or lack of insulin in the reservoir, circulating insulin concentration decrease suddenly and a hyperglycemic episode can occur (SELAM, 2010; SUBHASHINI, 2013).

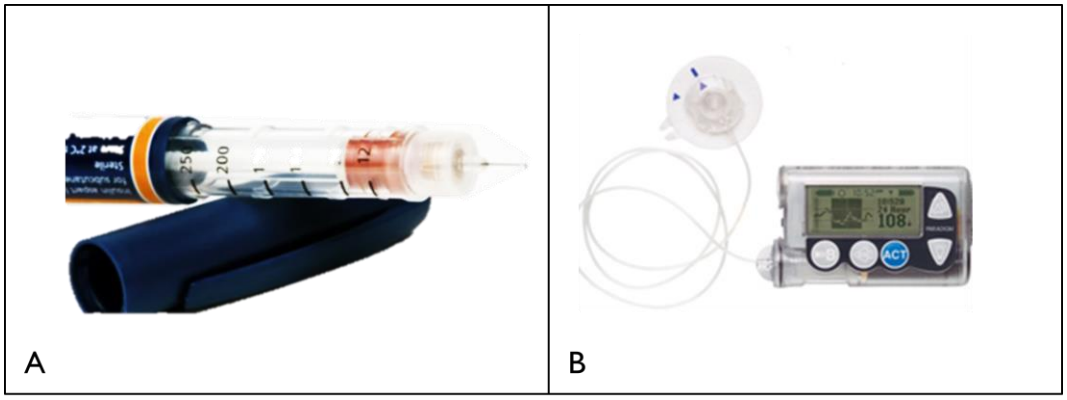


Figure 2 – Insulin delivery devices. A-Insulin pen system. Adapted from Diabetes Guide Today, 2014. B-Insulin pump. Adapted from Medtronic MiniMed Paradigm Insulin Pumps Lawsuit, 2014

Aerosol injectors (figure 3) deliver insulin in the mouth and they are still under development by the biotechnology industry. As well as the insulin inhalers, those are under consideration to insulin delivery due to large surface area of lungs (SELAM, 2010; SUBHASHINI, 2013).

Figure 3 - Aerosol insulin injector. Extracted from How to give an insulin injection, 2014

Jet injectors (figure 4) are developed to deliver insulin in a transcutaneous level at high speed and pressure to penetrate the skin without a needle. The insulin injected by this method is quickly absorbed but the repeated use of jet injectors potentiates a decrease of insulin absorption. Additionally, the use of this device is painful and its size and cost makes it unfavorably and often limits the routine use by patients (SELAM, 2010; SUBHASHINI, 2013).


Figure 4 - Insulin jet injector. Extracted from Pharmjet introduces needle-free subcutaneous and intramuscular injectors, 2014

Alternatively, the oral insulin administration could be ideal to the treatment of diabetes *mellitus* and even it does not replace the parenteral administration it will be certainly a complementary approach. The benefits of oral administration are many and have a wide range. In addition to patient adherence to the treatment be easier because oral administration is noninvasive, relatively free from complications and easily dosed, the exogenous insulin absorbed in the intestine can mimic much better the endogenous insulin, since in the bloodstream the insulin goes to the liver where it has a fundamental function (GORDON, 2002; CERNEA, 2006).

Considerations associated with developing effective oral formulations for proteins and peptides are generally attributed to their susceptibility to be degraded by luminal secretions, to their interaction with luminal membranes and to its contact with cytosolic enzymes before they can reach the bloodstream. Another concern is the metabolic activity of microflora in the lower small and large intestines, because bacterial colonies are capable of several metabolic reactions, such as deglucuronidation, decarboxylation, ester and amide hydrolysis, and dehydroxylation. Moreover, the poor intrinsic permeability of peptides and proteins to cross biological membranes as a result of their large molecular size, charge and protein hydrophilicity, limits their uptake through aqueous pores in the gut wall (GEISS, 2000; REIS, *et. al.*, 2006).

The oral administration of insulin has been largely studied. Based on these considerations, many possibilities have been considered, namely, (1) enzyme inhibitors in microparticles or nanoparticles (NP), whose usage has been questioned because of the long term toxicity (DAMGÉ, *et. al.*, 1997; QI, 2004; PEPPAS, 2006); (2) absorption promoters in capsules of gelatin, however the promoters' toxicity is not consensual and the disadvantage

is the nonspecific effect (TOUITOU, 1986; HOSNY, 1995); (3) use of liposomes, which, although its effectiveness has been proven in many fields of pharmaceutical technology, the results are strongly contradictory mainly due to its composition (SIMÕES, 2005); (4) use of NP, whose results are promising since its first approach by Oppenheim *et. al.* (1982).

NP are under consideration for oral delivery of proteins like insulin by stabilizing and ensuring biological activity during transit through the gastrointestinal tract and by facilitating delivery and absorption in the target site. Insulin absorption from the gastrointestinal tract into the portal vein would mimic the physiological route of insulin undergoing first hepatic bypass. Compared to parenteral delivery, less insulin would be necessary to obtain a therapeutic effect and, consequently, secondary effects due to high insulinaemia in extrahepatic tissues would be minimized. Besides this, NP prolong the permanence time of insulin in the intestine, which promotes high dispersion at the molecular level and consequently increases absorption (REIS, *et. al.*, 2006; WOITISKI, *et. al.*, 2009b).

## 1.2 Nanoparticles

NP as drug carriers are composed by natural, semisynthetic, or synthetic polymeric molecules of nanometer size which may or may not be biodegradable. NP are a collective name for nanospheres and nanocapsules. Nanospheres have a matrix-type structure; drugs or tracers may be absorbed at their surface, or entrapped or dissolved within the particle. Nanocapsules are vesicular systems in which the drugs are confined to a cavity or inner liquid core surrounded by a polymeric membrane (REIS, *et. al.*, 2006).

The size of NP is a main player regards its high intracellular uptake but also by its influence in intestinal absorption. The critical diameter to intestinal absorption of NP is 10μm as maximum limit; this factor is the most preponderant and it influences the biodistribution, the release profile and the mucoadhesive properties (GOMBOTZ, 1998; JUNG, 2000). Polymeric composition (hydrophobicity, surface electric charge and biodegradation profile), nature of adjuvants and drugs (molecular weight, charge and localization on nanoparticle) have high influence in NP absorption, distribution, metabolism and elimination. Thus, the design of NP involves interconnected processes toward developing and optimizing NP formulation, based on physicochemical, pharmacological and physiological parameters. Considering that, the design of NP for orally dosed insulin is a promising approach for the treatment of diabetes *mellitus*, attempts include the use of biomaterials that have demonstrated favorable characteristics for protein entrapment, absorption across the intestinal membrane and delivery to the target site (JUNG, 2000; REIS, *et. al.*, 2006; WOITISKI, *et. al.*, 2009b).

Many have been the approaches used in the development of NP for oral delivery of insulin. There are many compounds available to use in NP formulation, such as polyisobutylcyanoacrylate (PIBCA), poly(alkylcyanoacrylate) (PACA), poly(methylmethacrylate) (PMMA), polylactic acid (PLA), poly(lactic-co-glycolic acid) (PLGA) and others, which results have showed hypoglycemic effect in diabetic mice (HANEMANN, 2012; JAWAHAR, 2013). Nowadays, the feed lines in nanotechnology are directed to the use of natural polymers. Actually, polymers derived from natural and renewable sources are increasingly interesting to pharmaceutical industry due to its biocompatibility, biodegradability, gelation possibility, and easy, quick and accessible acquisition. There are several polymers with these characteristics, like agar, agarose, carrageenan and alginate. Among these polymers, alginate is the most advantageous and has become increasingly important in many areas. A higher number of studies have been carried out with this polymer; however, the optimization of the formulation that are related with the size of the particles obtained, the efficiency of encapsulation, the bioavailability and the hypoglycemic effect achieved *in vivo* studies are the major difficulties to overcome (ONAL, 2002; CUI, 2004; SILVA 2006).

### 1.2.1 Alginate

Pharmaceutical industry has used a matrix-alginate to encapsulate several drugs. This choice is related to alginate ability to form a gel in the presence of multivalent cations with compatible conditions with encapsulated drugs. Another advantage of alginate is that it undergoes partial degradation in human gastrointestinal tract which makes it similar to soluble dietary fiber, and it is also free of toxicity and immunogenicity (GOMBOTZ, 1998; BURTING, 2003; WOITISKI, *et. al.*, 2009b). In addition, alginate has bioadhesive properties due to a high quantity of carboxyl groups that establish hydrogen bonds with mucus intestinal glycoproteins, which is an advantage to delivery drugs in the intestine. Besides, the sensibility of alginate to pH changes allows the release of encapsulated drugs (WOITISKI, *et. al.*, 2009b).

Alginate is a natural polymer extracted from brown algae (*Phaeophyceae*), being one of the most available polymers, and to commercial purpose *Macrocystis pyrifera*, *Laminaria hyperborean* and *Ascophyllum nodosum* are the most used species to extract alginate (Gombotz 1998). Alginate consists of a polysaccharide of anionic chains not branched with two types of polyuronic acid, the β-D-mannuronic acid (M) and α-L-guluronic (G) acid linked by (1,4) glycosidic bonds. These monomeric units can naturally appear in three different

combinations (figure 5), heteropolymeric units (MGM) or monomeric units (GGG or MMM) (LIU, 2002a; WOITISKI, *et. al.*, 2009b).

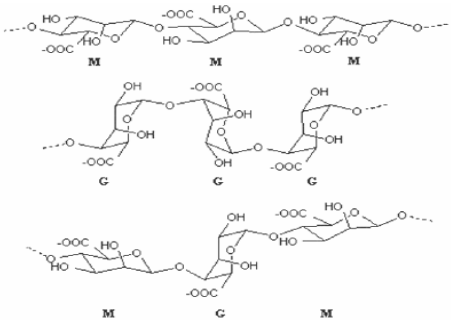

Figure 3 – Alginate structure, G and M residues. Extracted from Liu 2002a.

Alginate has gelling properties that allows the formation of two kinds of gel, an acid gel and an ionotropic gel. The ionotropic gel is formed in the presence of some divalent and trivalent cations and can retain in the core, drugs or other compounds.

The alginate composition should be considered in the gelling phase because it has a big influence in intumescence and its availability to encapsulate drugs. During the gelling, cations binds preferentially to guluronic residues, thus the content of these residues affects the hardness, the porosity, the stability and the elasticity of gel, and the size and shape of the particles formed (GOMBOTZ, 1998; PONCELET, 2001; SARMENTO, *et. al.*, 2007a).

Alginate is a hydrophilic polymer with slow dissolution in cold water, but once dissolved originates viscous colloidal solutions. The solubility of alginate in aqueous solution is determined by the cations and other compounds present in the solution, temperature and pH changes. Concerning pH, when pH is higher than its $pK_{a,}$ alginate is negatively charged and its hydration occurs. On the other hand, when pH is lower than the $pK_a$ of alginate (3.38 and 3.65 to mannuronic and guluronic residues, respectively) it precipitates in the form of alginic acid (SHILPA, 2003).

Sodium alginate used in nanoencapsulation techniques should have a concentration between 1-3% (m/v). If alginate's concentration is lower than 1% (m/v) the carboxylic groups are insufficient to form spherical particles during the gelling (SARMENTO, *et. al.*, 2007a). If the concentration of alginates is above 3% (m/v), viscosity increases and consequently the size of the obtained particles increase as well (LIU, 2002a).

Basically, alginate forms a stable and reversible hydrogel in the presence of multivalent cations due to intramolecular and intermolecular cross-linking, resulting in compact coiled chains of a pre-gel state. Calcium is a cation widely used in the gelling process of alginate, because it is safe to clinical applications, easily available and cheap. However, other divalent cations, such as $Sr^{2+}$ (strontium) and $Ba^{2+}$ (barium) and trivalent cations, such as $Fe^{3+}$ (iron)

and $Al^{3+}$ (aluminum) can also be used, but monovalent cations and $Mg^{2+}$ (magnesium) are not able to form alginate gel (RAJAONARIVONY, 1993; GOMBOTZ, 1998; WOITISKI, *et. al.*, 2009a).

In the mechanism of gelling alginate the interactions occur preferentially between calcium ions and guluronic units making a strong and thermostable gel, whose properties depend on the polymer characteristics and the NP preparation method. Calcium bonds to alginate by electrostatic interactions but also by bonding to 7-9 atoms of oxygen to carboxyl and hydroxyl groups of four different monomers. Furthermore, each alginate chain can dimerize to form junction zones trough bonds between polysaccharide chains making a solid gel and this is possible due to calcium quelation (GOMBOTZ, 1998; SHILPA, 2003). A few salts of calcium can be used, such as oxalate, tartrate, phosphate, carbonate and citrate. Among these salts, carbonate of calcium shows the best results because obtained NP are spherical, have unimodal size distribution, stable, and remain stable in a wide pH range (PONCELET, 2001). The grain size of calcium salt has a big influence on NP aspect, size and resistance. As lowest the size of the grain calcium salt is, the bigger will be the calcium ion quantity widespread between the chains of alginate and the gel will be much more stable (PONCELET, 2001).

## 1.3 Insulin-NP

NP studied in this work were formulated by emulsification/internal gelation. They were described as a multilayer complex with the insulin protected and retained within the nanoparticle which had an outermost coat consisting of a protease-protective protein. The nucleus' particle consists of calcium cross-linked alginate, dextran sulfate and insulin following complexation with chitosan and outermost coated with bovine serum albumin. The figure 6 shows a schematic representation of this NP. (WOITISKI, *et. al.*, 2009a; WOITISKI, *et. al.*, 2009b).

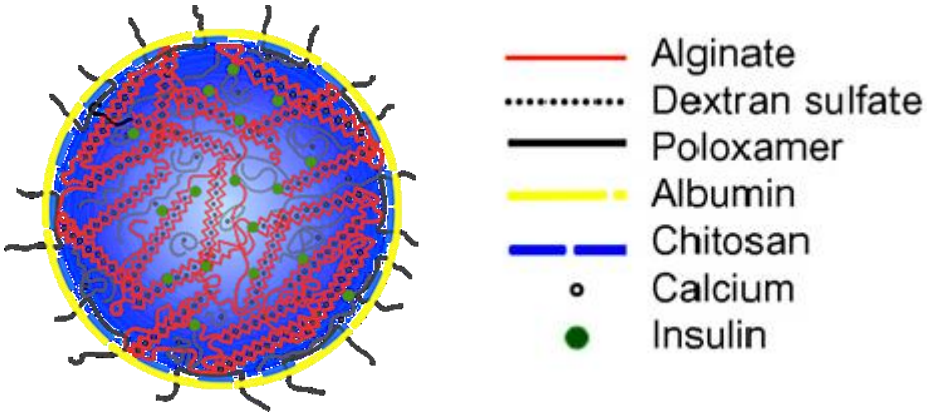


Figure 6 – Schematic representation of multilayered NP encapsulating insulin. NP are formulated by calcium cross-linked alginate, dextran sulfate and insulin following complexation with chitosan and outermost coated with bovine serum albumin. Adapted from WOITISKI 2010.

The production method of polymeric network designated internal gelation was developed with alginate as base polymer. It consists of a mixture of sodium alginate and a calcium complex, and, by decreasing pH, the calcium ion is released from the complex and reacts with alginate. This method was adapted to produce particles in gel, to turn over the toxic products resulting, and currently is designed by emulsification/internal gelation (LIU, 2002a).

### 1.3.1 Emulsification/internal gelation

The emulsification/internal gelation method involves the preparation of an insoluble salt calcium suspension in an alginate solution. This mixture is scattered in oil, in the presence or absence of emulsifier agent, and the result is a W/O (water in oil) emulsion. After this, the calcium salt is dissolved by the addition of an acid and the alginate gelation occurs by reticulation with calcium ions. The oil used in emulsification/internal gelation method can be obtained from nature (e.g. corn, peanut and soybean) or minerals (e.g. paraffin oil, isooctane oil and silicon). The ratio of aqueous phase and oil phase has influence in the size of the particles formed, and it is typically between 1:1 and 1:5 (v/v) (LIU, 2002a).

The emulsifier agent has two functions in the emulsification process, the decrease of the surface tension facilitating the dispersion of aqueous and oil phases and the surface stabilization avoiding the coalescence of the droplets. One of the most important aspects of the emulsifier agent is the ability to quickly form a film around of each droplet of internal phase, avoiding its coalescence when they come into contact with each other'. In emulsification/internal gelation process several emulsifier agents have been tested, such as, lecithin, sorbitan monooleate (Span® 80), sorbitan trioleate (Span® 85) and, polyoxyethylene sorbitan monooleate (Tween® 80) (LIU, 2002a; LIU, 2002b).

The emulsifier agent concentration is a very important factor in the emulsification/internal gelation method. When it is too low (<0.5%, v/v) the film formed around the droplets can be incomplete decreasing droplets stabilization. On the other hand, concentrations higher than 2.0% (v/v) can cause resistance to pH reduction, increasing the gelation time that decreases the process income (LIU, 2002b). When one acid is added to the oil and it scatters in the aqueous phase, pH decreases immediately, and then the calcium complex solubilizes and the cations are available to alginate gelation. The acid concentration should be studied and controlled to obtain the desire effect without damaging the agent to encapsulate. There are a few acids soluble in oil suitable to emulsification/internal gelation process, such as, acetic acid, citric acid and lactic acid (LENCKI, 1989).

To sum up, the emulsification/internal gelation method is safe, simple and economic. The low stress of the process allows the use of very sensible agents. Furthermore, a homogeneous gel is obtained and the size of the particles can be controlled. On the other side, the porosity of particles obtained can be a limiting factor, because it can decrease the entrapment efficiency and increase the velocity of release of encapsulated agent in gastrointestinal fluid. All these factors should be considered in the design of NP obtained by this technique (PONCELET, 1992; VANDENBERG, 2001).

Transposition of this method for industrial scale could be easy because it is possible to produce a large number of particles without highly sophisticated equipment. *Poncelet et al.* (1992) studied the equipment influence in NP size and in the batch yield, regarding two factors, the reactor geometry and the impellers type. Thus, a round bottom reactor increases the income of the batch because it avoids the appearance of dead volumes during agitation and, consequently, alginate solution accumulates and forms aggregates. In respect to impellers type, the marine impeller showed the best results when compared with the impeler network, due to lower adhesion and aggregation performed. Furthermore, the marine propeller allows a higher homogeneity when compared with six turbine blades.

The recuperation of the NP scattered in the W/O emulsion should be performed with appropriate wash. Usually this is achieved adding an aqueous washing medium that perturbs the W/O emulsion equilibrium causing the phases inversion. It allows the migration of the NP from the oil phase to aqueous phase. The recuperation factors should be strictly controlled because there is a risk to form very stable O/W (oil in water) emulsion precluding the recuperation of NP (ARSHADY, 1990; PONCELET, 1992). There are several aspects to consider in the recuperation process, such as, NP size and shape, oil elimination easiness, number of wash cycles, recuperation income, entrapment efficiency, insulin release profile and physic-chemical stability of encapsulated insulin (PONCELET, 1992).

### 1.3.2 Reinforce the alginate matrix

Considering nanoencapsulation, the entrapment efficiency is very important and at this point the emulsification/internal gelation method has a disadvantage due to insulin release in acidic medium. As mentioned above, NP should have ability not only to encapsulate insulin but also to release the encapsulated agent, only in target site. Thus, a way to control the release profile is to add other polymers to alginate matrix. The polymers to reinforce alginate matrix must have negative charge because it is the same charge of alginate, so the formation of complexes between these two polymers is almost unlikely. If alginate interacts with a second polymer and it forms a complex, the insulin entrapment will be conditioned.

On the other side, adding an anionic polymer could increase the insulin entrapment on alginate matrix because the matrix stays denser and the insulin diffusion becomes difficult. Besides, insulin-anionic polymer interaction forms a polyelectrolyte complex that is reversible which is an advantage to release insulin in its native conformation (CHAN, 1997).

Additional incorporation of dextran sulfate improves insulin entrapment efficiency and it modulates insulin release from NP (WOITISKI, *et. al.*, 2009a). Dextran sulfate is a branched chain polymer with biodegradable and biocompatible properties. It has low molecular weight (5kDa) and it is a strong anionic polymer that contains 2.3 sulfate groups per glycosyl residue. Sulfate dextran interacts with isolated ions, like calcium, and polycationic polymers. This polymer has high purity and stability and it is very useful to selectively precipitate lipoproteins, to hybridization reactions, and to protein stabilization reactions. As hydrophilic polymer can contribute to water-soluble proteins encapsulation, and it can also promotes longer periods of circulation *in vivo* (REIS, 2008; WOITISKI, *et. al.*, 2009a; WOITISKI, *et. al.*, 2009b).

### 1.3.3 Insulin-NP coating

Alginate and chitosan NP have been widely used and extensively reported for oral delivery of insulin. Chitosan is positively charged and consequently it is used for the incorporation of other polyanionic polymers to modulate insulin entrapment, stability, retention and release in the gastrointestinal tract (WOITISKI, *et. al.*, 2009a; WOITISKI, *et. al.*, 2009b).

Chitosan is an unbranched polyamine of D-glucosamine and *N*-acetyl glucosamine with mucoadhesive, biodegradable and biocompatible properties and it can be derived by partial deacetylation of chitin from crustacean shells. It has potential to reduce transepithelial electrical resistance and transiently opens tight junction between epithelial cells to enhance insulin absorption via paracellular pathway (WOITISKI, *et. al.*, 2009a; WOITISKI, *et. al.*, 2009b). Chitosan is important to stabilize the alginate hydrogels in the formation of NP, reinforcing the fragile alginate nucleus, due to its pH-sensitive behavior. It is soluble at low pH due to protonation of amino groups and insoluble at higher pH values. The acid type used to dissolve chitosan influences the stability, strength, mucoadhesive and disintegrating properties determining the physicochemical properties of NP. Lactic acid is normally used to dissolve chitosan and provides greater bioadhesive and flexible elastic properties than chitosan dissolved in acetic acid (WOITISKI, *et. al.*, 2009a; WOITISKI, *et. al.*, 2009b).

Stabilizers are important to modulate the structural properties of NP with high tendency to aggregate by providing stability in suspension and influencing interaction

between particles and enzymes, and cells and its membranes. Steric stabilization of NP is induced by poloxamer 188 that is a nonionic triblock copolymer composed of a central hydrophobic chain of polypropylene oxide and two hydrophilic chains of polyethylene oxide. Poloxamer is bound to the nanoparticle surface by hydrophobic interaction of the polyethylene oxide chains with methyl groups of chitosan, while the hydrophilic polyethylene oxide chains protrude into the surrounding medium to create a steric barrier. Poloxamer reduces particle aggregation and enzyme adsorption in gastrointestinal tract, which may interfere with the nanoparticle carrier function by degrading insulin (WOITISKI, *et. al.*, 2009b).

Additionally, improvement of insulin protection against enzymatic degradation represents an essential strategy in the successful oral administration of insulin-based NP. Factors that counteracted the pharmacological effect of orally dosed insulin were calculated as 60% due to insulin degradation, 23% due to premature insulin release and 17% due to lack of mucoadhesion. By these factors**,** albumin coating is designed to minimize acid degradation and to prevent proteases from accessing insulin within the nanoparticle, acting as a sacrificial target to enzymatic degradation (WOITISKI, *et. al.*, 2009b).

#### 1.3.3.1 Albumin

The albumin has widely been studied and has several applications at pharmaceutical industry. Considering the nanotechnology, the albumin has been used in three different ways, as drugs model to be encapsulated, as main polymer to encapsulate other drugs and, as coating polymer at polymeric NP. In this work, as previously mentioned BSA is used to coat NP. This choice is based in other works that showed an increase in the stability of alginate-NP and has a protecting effect on insulin (HURTEAUX, 2005; SCHECHTER, 2005).

Serum albumins are the most abundant soluble circulatory proteins in the blood (52-60% of plasma) of mammalians and they are exclusively synthesized by the parenchymal cells of the liver. The half-lives are variable and the bovine serum albumin has a half-life of 19 days. Serum albumin is crucial to maintaining plasma volume and the osmotic pressure of circulating blood. In addition, it also has function as carrier for hormones, enzymes, fatty acids, bilirubin, metal ions, and medicinal products to the target tissues. The albumin helps in the metabolism and affects the pharmacokinetics of many drugs, reduces the activity of toxins, acts as free-radical scavenger and sometimes displays pseudo-enzymatic properties (WANG, *et. al.*, 2007; WANG, *et. al.*, 2011).

Human serum albumin (HSA) is a globular protein with a single polypeptidic chain, consisting of 585 amino acid residues. It contains low quantities of tryptophan and high cysteine's quantities and its secondary structure consists in α-helix having six turns and seventeen disulphide bridges. Bovine serum albumin (BSA) shares approximately 76% sequence homology with HSA (figure 7), which is also a single polypeptidic chain with 583 amino acid residues. BSA has seventeen disulphide bridges, as well, and one free -SH group, which makes possible the formation of a covalently linked dimer. These proteins are charged amino acid residues with apolar surface, and their interior is almost hydrophobic, in nature. Besides, BSA is characterized by three domains, each consisting of a large and a small double loop and a short and a long connecting segment. The major difference between HSA and BSA is that the first is human and contains only one tryptophan amino acid residue while the latter is bovine and has two residues. BSA has an isoelectric point of 4.7 while HSA has the isoelectric point of 5 (URBANO, 2004; AKDOGAN, 2012).

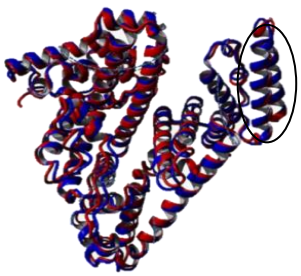

Figure 7 –Crystal structure aligment of HSA (blue) and BSA (red). Adapted from Akdogan 2012.

Usually, the plasmatic proteins are not internalized by the cells, which use plasmatic amino acids to produce their proteins. Thus, albumin and the other plasmatic proteins perform its functions in the plasma or interstitial fluid. Once synthesized, albumin molecules are secreted into the blood stream and extravasate from the intravascular space to the interstitial space. Apparently, albumin breakdown occurs directly from the intravascular compartment, probably by the endothelial cells. The kidney degradates about 10% of albumin and more than 10% seems to be leaking into the gastrointestinal tract. Albumin present in the interstitial space returns by the lymphatic flow back to the intravascular compartment (URBANO, 2004).

## 1.4 Insulin-NP characterization

To optimize formulation of NP several parameters should be taken in account, such as their size distribution, polydispersity index, zeta potential, insulin entrapment efficiency, insulin release in gastric and intestinal simulation conditions and *in vivo* pharmacological activity (SARMENTO, *et. al.*, 2007b; WOITISKI, *et. al.*, 2009b).

### 1.4.1 NP size

NP average diameter is dependent upon NP composition, mainly the concentration of calcium chloride, chitosan, and albumin. Calcium concentration affects significantly the NP size and, intramolecular cross-linking of individual alginate chains ledding to a pregel state and compact coiled structure, but an increase calcium concentration results in gel aggregation and consequently the formation of bigger particles. Chitosan complexation contributes to the alginate nucleus size in proportion to its initial diameter, since larger nuclei have more carboxylic groups to interact with amino groups of chitosan. The albumin concentration effect on decreasing nanoparticle diameter, possibly related to a reduction in the electrical repulsion among biopolymers, where modifications in the electrical state cause swelling or shrinking of the particle, depending on whether the electrical repulsions increase or decrease, respectively (WOITISKI, *et. al.*, 2009a; WOITISKI, *et. al.*, 2009b).

Polydispersity index represents the size distribution, and the mean value decreases when calcium chloride concentration is low, however it does not depend on chitosan or albumin concentrations. Calcium reduces nanoparticle aggregation that results in a narrower but polydisperse particle size distribution (WOITISKI, *et. al.*, 2009b).

### 1.4.2 Zeta potential

Zeta potential lower than -30mV which shows higher electrostatic stabilization of NP in suspension, whereas large repulsive forces prevent aggregation upon random impact of adjacent NP. It is an important parameter for insulin physicochemical and biological stability. The negative zeta potential shows the prevalence of negative charges suggesting the presence of albumin on the nanoparticle surface that interacts with positively charged chitosan at a pH above the albumin isoelectric point (WOITISKI, *et. al.*, 2009a; WOITISKI, *et. al.*, 2009b).

### 1.4.3 Entrapment efficiency

Entrapment efficiency of insulin it is influenced by many factors. High insulin entrapment values were obtained with high concentrations of calcium chloride (0.24%), which can be explained by ionic bridges established between carboxylic residues of insulin amino acids and alginate chains when calcium ions interact with guluronic residues of alginate, and consequently the insulin association to alginate nucleus is enhanced (WOITISKI, *et. al.*, 2009b). Entrapment efficiency is higher to lower albumin concentrations (0.25% and 0.50%), because the addition of albumin solution at pH 5.1 raises the pH of the nanoparticle suspension to the isoelectric point of insulin, decreasing the electrostatic interaction strength between insulin and alginate/dextran sulfate nucleus. The lowest entrapment

efficiency is obtained with a low calcium chloride concentration and a high albumin concentration (WOITISKI, *et. al.*, 2009b).

### 1.4.4 Release profile *in vitro*

Insulin release in enzyme-free simulated digestive fluids was carried out to define insulin retention within NP and its ability to prevent insulin from acid degradation. Insulin release is influenced by NP' swelling based on chitosan properties at low pH that facilitates the diffusion of ions present in the simulated gastric fluid inside them, breaking the ionic interaction between insulin and nanoparticle nucleus. Thus, high concentration of chitosan increases insulin retention, as well as high concentration of albumin results in higher insulin release, likely due to a weakening of electrostatic interaction between insulin and the alginate/dextran nuclei, which is reliant to pH conditions (WOITISKI, *et. al.*, 2009a; WOITISKI, *et. al.*, 2009b).

Ideally, insulin remains associated with NP in gastric conditions, and it is only released at the intestinal pH where the absorption potential is optimal. After gastric simulation, NP were transferred to enzyme-free simulated intestinal fluid and high levels of cumulative insulin release take place after 180 minutes in the simulated intestinal fluid (SARMENTO, 2007a). Thus, it appears that pH triggers insulin release, potentially as NP pass from the acidic gastric medium, into a neutral intestinal medium, which can be attributed to electrostatic repulsion between alginate and insulin, both staying negatively charged. Moreover, dissolution of the alginate nucleus, as a result of calcium loss and alginate swelling, can happen. This combined with the mucoadhesive properties of alginate and chitosan, which stay exposed after degradation of the sacrificial-target albumin in the stomach, would result in adhesion of the NP to the intestinal mucosa to release insulin directly at the site of absorption (SARMENTO, *et. al.*, 2007a; SARMENTO, *et. al.*, 2007b; WOITISKI, *et. al.*, 2009a; WOITISKI, *et. al.*, 2009b).

### 1.4.5 *In vivo* characterization

The pharmacological effect of insulin-NP was evaluated in a work (SARMENTO, *et. al.*, 2007b) performed by oral administration of NP (50 and 100 IU/kg of insulin) in diabetic rats, which changes in plasma glucose were compared with subcutaneously administration of free insulin at 2.5 IU/kg and orally administration of empty NP, and the results showed an effective decrease of the blood glucose levels at administrated doses by insulin-NP.

A crucial issue for successful development of this therapy is to understand and control the biodistribution of NP, which can provide valuable information early in the development of this approach. This importance has created a demand for techniques that can analyze the

information not only qualitatively but also quantitatively. Biodistribution studies can be carried out in animals by measuring the radioactivity of labelled compounds by nuclear medicine techniques. It gives an indication of global tissue accumulation patterns, which helps the design and the optimization of formulation. In addition, the ability to provide non-invasive, three dimensional and quantitative data inherent to nuclear medicine has become a relevant assay for biologic characterization, to drugs screening, optimization and biological safety (LIU, 2012; McCONVILLE, 2013).

## 1.5 Nuclear Medicine

Nuclear medicine is defined as a medical specialty that uses unsealed sources of radiation in the diagnosis and treatment of diseases. The role of nuclear medicine in clinical diagnosis is due to its ability to detect function with great sensitivity generating a functional image that shows the body´s biochemistry, taking in account the radiopharmaceutical chosen. For this reason nuclear medicine has contributes not only to clinical diagnosis but also to the understanding of disease mechanisms (LENTLE, 2003; SHARP, 2005). In nuclear medicine, functional information is resulted from the distribution of a radiopharmaceutical administered to the patient, usually by intravenous injection. By labelling a pharmaceutical with a radionuclide, the biodistribution of this radiopharmaceutical can be measured, only by the amount of radioactivity present (SHARP, 2005). Thus, nuclear medicine is a technique that is intrinsically functional because it measures the radiation emitted by a tracer specific to a particular function and, therefore, the location and concentration are directly related to the specific function (LENTLE, 2003). A radiopharmaceutical is a radioactive compound, without or with a minimal pharmaceutical effect due to low concentration that is used. Thus, it is used in nuclear medicine for diagnosis and treatment of human diseases, however 95% of the radiopharmaceuticals have a diagnostic purpose (SAHA, 2004a). The usefulness of a radiopharmaceutical is dictated by the characteristics of the radionuclide and the pharmaceutical. In a radiopharmaceutical design, the pharmaceutical is chosen on the basis of its preferential localization in a given organ or its participation in a specific physiologic function. After, a suitable radionuclide is added to the chosen pharmaceutical to form a radiopharmaceutical which after administration will emit radiations that are detected by a external radiation detector. Thus, the physiologic function and sometimes the morphologic structure of the organ or system can be assessed. Radiation from the radionuclide chosen should be easily detected by nuclear medicine instruments, and the radiation dose to the patient should be as low as reasonable available, according to ALARA principle. A radiopharmaceutical should obey some characteristics, such as easy availability, short

effective half-live, high target non-target activity ratio and radioisotopes adequate for the purpose, γ-rays emitters are preferable to image acquisition in conventional cameras-gamma, positron emitters are used to positron emission tomography (PET) acquisitions and α and β emitters are useful for the therapeutic purpose (SAHA, 2004a).

### 1.5.1 Nuclear Medicine Techniques

The term "nuclear medicine" comprises different imaging techniques ranging from PET and single photon emission computed tomography (SPECT) through a whole body planar images or "scans" (LENTLE, 2003).

Nuclear medicine images are generated by the detection of gamma-rays, X-rays or annihilation quanta. The cameras crystals detect the density of gamma-rays emitted per unit area and in the case of single photon emitters the direction of flight is determined by geometric collimation (SAHA, 2004a).

Scintigraphic instrumentation consists of scintillation crystals to convert gamma-ray into visible light, suitable light sensors (photomultiplier tubes), readout electronics and image processing units. Scintillators emit light after the gamma photon has deposited its energy in the crystal. NaI(Tl) (sodium iodide with thallium doping) scintillation crystal is often used in nuclear medicine because of its high light output, reasonable decay time that makes this crystal the choice for single photon detection with energies of 70-360keV (detection efficiency of 90% for 140keV) (MAHER, 2004; SAHA, 2004a).

Since the emission of gamma-rays is isotropic, collimation is needed to restrict data to gamma-rays of defined directions. Collimator design always is a balance between spatial resolution and sensitivity: reducing the size of the holes or using longer septa improves spatial resolution but reduces sensitivity at the same time. This fact is the most important tradeoff in the imaging process using Anger cameras (MAHER, 2004).

Positron emission tomography (PET) utilizes the unique feature of two high-energy annihilation-rays emitted back-to-back after positron interaction. Detector pairs count all events which occur in both of them within a very short time interval (10-20 ns). From data along these lines of response, the distribution of radioactivity can be reconstructed by mathematical methods (MAHER, 2004; SAHA, 2004b).

Therefore, as previously mentioned, radionuclide is chosen depending on the image technique. For PET acquisition, the most used positron emitter is $^{18}F$, and its use to label Fluorodeoxyglucose (FDG) has propelled this technique. This radiopharmaceutical allows to evaluate cells glycolytic activity, since it is a glucose analogue. Thus, $^{18}F$-FDG uptake in cells reveals its viability and proliferation rate. The accurate of the PET/CT with $^{18}F$-FDG make

this radiopharmaceutical the gold standard for oncologic applications. Besides, $^{18}$F-FDG has first used in neuroscience and cardiology (COLEMAN, 2006). The search for new radiopharmaceuticals for PET images have widely increase and other radiopharmaceuticals have been approved for myocardial perfusion, like $^{82}$Ru and $^{13}$N-ammonia, for protein synthesis, such as $^{11}$C-acetate, and for neuroendocrine tumors, such as $^{68}$Ga-DOTATATE ($^{68}$Ga-DOTA-$_D$Phe,$^1$Tyr$^3$-octreotate) (JADVAR, 2005; KAYANI, *et. al.*, 2008).

The conventional nuclear medicine has application in all of biologic systems and the radiopharmaceuticals routinely used to clinical diagnostic are assorted. In this field many radionuclides are used, such as, $^{201}$Tl, $^{123}$I, $^{67}$Ga, $^{111}$In and $^{99m}$Tc. Among these radionuclides, technetium-99m is the most attractive to the nuclear medicine physician because of its optimal gamma energy for SPECT, its availability, its relatively low cost, and its easy-to-label kit preparations for in-house use. Another advantage is the low radiation burden to patients, due primarily to its short half-life. Ideally, the half-life should not be very short to avoid that the activity have decayed to a very low levels before the image begin. On the other hand, if it is too long the patient will remain radioactive for a considerable time and in order to reduce the possibility of radiation damage the amount of activity administered should be kept low. The decay within hours also facilitates the handling of waste (PERSSON, 1969; YOKOYAMA, *et. al.*, 1975; SHARP, 2005).

### 1.5.2 $^{99m}$Tc-radiopharmaceuticals

The $^{99m}$Tc-labeled compounds constitute more than 80% of radiopharmaceuticals used in clinical nuclear medicine. Technetium is a transition metal of VIIB group of the periodic table, it has an atomic number of fourty-three and it was discovered in 1937 by Perrier and Segré. There are twenty-five isotopes and ten isomers of technetium and the $^{99}$Tc is the most common. This isotope decays by $\beta^-$ emission with 293KeV of energy and $2{,}13 \times 10^5$ years of half-life (SAHA, 2004a).

The technetium-99m is a radionuclide often used in single photon emission Nuclear Medicine due to its several physical and chemical factors such as approximate monoenergetic gamma decay (140 - 142 keV), high photon flux detected efficiently by the NaI(Tl) crystals of the gamma-cameras which allows image acquisition with good resolution. Technetium-99m is a nuclear isometric state of technetium-99 with a half-life of 6.01 hours, that also represents a favorable characteristic for the patient dosimetry (MAHAMOOD, 2003; SAHA, 2004a; DESCRITOFORO, 2007).

The technetium-99m is an artificial element obtained by $^{99}$Mo/$^{99m}$Tc generator in which $^{99}$Mo ($t_{1/2}$=65.94 hours) decays to $^{99}$Tc. This radionuclide system made technetium-99m

available for clinical use and research and has stimulate the development of compounds with considerable impact on radiochemistry and nuclear medicine. An efficient separation makes possible to obtain $^{99m}Tc$ with high specific activity in aqueous solution as sodium pertechnetate ($Na^{99m}TcO_4^-$), represented in figure 8. The pertechnetate ion is obtained in a +7 oxidation state; with a tetrahetral geometry, the $Tc^{+7}$ stays in the center and the oxygen in each vertex of tetrahedron.

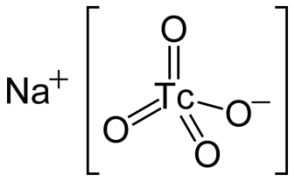


Figure 8 – Schematic representation of chemical formula of $Na^{99m}TcO_4^-$. Exported by Saha, 2004a.

Thus, this oxidation state of technetium does not promotes the formation of complexes with chelates or ligands which makes necessary to reduce it (SAHA, 2004a; DESCRITOFORO, 2007). Eight oxidation states (-I to VII) are possible, and the most stable states are (VII), (V), (IV), (III), (I) and (0), and these states, conjugated with several coordination geometries, confers to this compound a rich and versatile chemistry (RHODES, 1974; BANERJEE, 2001; MAHAMOOD, 2003). The majority of $^{99m}Tc$ radiopharmaceuticals contains technetium as Tc(V) (SAHA, 2004a; DESCRITOFORO, 2007).

Concerning $^{99m}Tc$ radiopharmaceuticals applications, there are perfusion agents, such as $^{99m}Tc$-MIBI ($^{99m}Tc$-methoxyisobutyl isonitrile) for myocardium perfusion or $^{99m}Tc$-ECD ($^{99m}Tc$-ethyl cysteinate dimer) for brain perfusion; bone agents such as $^{99m}Tc$-diphosphonates; renal agents, such as $^{99m}Tc$-DTPA ($^{99m}Tc$-diethylenetriaminepentaacetate) and $^{99m}Tc$-$MAG_3$ ($^{99m}Tc$-mecraptoacetyltriglycine); lung agents, such as $^{99m}Tc$-MAA ($^{99m}Tc$-macroagregates of human serum albumin); and oncologic agents, such as $^{99m}Tc$-diphosphonates often used for bone metastasis, $^{99m}Tc$-HSA nanocolloid ($^{99m}Tc$-human serum albumin nanocolloid) for sentinel lymph node scintigraphy (ZOLLE, 2007).

Along the years many have been the radiopharmaceuticals approved for use in nuclear medicine, but, one the other hand, there are radiopharmaceuticals that are used anymore, such as $^{99m}Tc$-HSA. Biodistribution of HSA labeled with technetium-99m after intravenous administration had a similar behavior to the patient's own serum albumin and served as a suitable tracer for the vascular compartment. Eventually, labeled albumin could be used for studies of nuclear angiography, gated cardiac blood-pool, albumin metabolism, direct placental visualization, cisternography and gastrointestinal-blood-loss, and it was readily available in the end of the 60´s and beginning of the 70´s (PERSSON and LIDÉN 1969;

RHODES, 1974). Plasma-derived HSA (pHSA) was clinically used to correct circulating plasma volume and improve colloid osmotic pressure. Nevertheless, pHSA supply was limited as it was manufactured from a fractionation of donated human plasma. This nonautologous multisource approach introduced significant risks of allergic reactions and contamination by blood-derived pathogens, such as human immunodeficiency virus (HIV), viral hepatitis, and Creutzfeld-Jakob disease prions (WANG, *et. al.*, 2011). For these reasons the nuclear medicine studies with albumin were abandoned (RHODES, 1974; WANG, *et. al.*, 2007). Although, the HSA is again available to nuclear medicine applications, $^{99m}$Tc-HSA was replaced by $^{99m}$Tc-RBC ($^{99m}$Tc-red blood cells) for nuclear angiography and by cardiac agents for the gated cardiac blood-pool (ZOLLE, 2007).

### 1.5.3 Albumin radiolabeling

Protein binding is greatly influenced by a number of factors, such as its charge, pH and nature. The nature of a protein, particularly its content of hydroxyl, carboxyl, and amino groups and their configuration in the protein structure, determines the extent and strength of its binding to the radioisotope. In general, in a radiolabeling procedure should be into account the compatibility between the drug and the isotope, the stability, the solubility, the biodistribution, plasmatic proteins binding, the size and the charge of the drug (SAHA 2004a). In an isotope exchange reaction, one or more atoms in a molecule are replaced by an isotope of the same element, having different mass numbers. Since the radiolabeled and parent molecules are identical except for the isotope effect, they are expected to have the same biologic and chemical properties (SAHA, 2004a).

Yuh-Feng Wang *et. al.* have been developed a $^{99m}$Tc-HSA preparation technique using autologous albumin, which was radiolabeled by stannous chloride method (WANG, *et. al.*, 2007; WANG, *et. al.*, 2011). As previously mentioned, chemically, $Na^{99m}TcO_4^-$ is a nonreactive specie and does not label any compound by direct addition. In $^{99m}$Tc-labeling of many compounds, prior reduction of $^{99m}$Tc from the 7+ state to a lower oxidation state is required. Various reducing agents have been used, such as stannous citrate, stannous tartrate, concentrated hydrochloride acid (HCl), sodium brohydride, dithionite, ferrous sulfate and stannous chloride. Among these, stannous chloride is the most commonly used reducing agent used in the most preparation of $^{99m}$Tc-labeled compounds. The oxidation state of technetium in $^{99m}$Tc-HSA is not known with certainty, but has been postulated to be 5+ (SAHA, 2004a). The advantages of stannous salts for kit formulation have been demonstrated, and the stability of kits was increased by their lyophilization because stannous salts are nontoxic and stable when lyophilized and kept in a nitrogen atmosphere. The

feature that makes it so interesting for $^{99m}$Tc-radiopharmaceutical preparation is the easiness of the stannous ion ($Sn^{2+}$) to be oxidized to tin (IV) according to the reaction:

$Sn^{2+} \rightarrow Sn^{4+} + 2e^-$

The amount of stannous chloride is empirically optimized for each individual kit formulation, maintaining the balance between two parameters: (1) a large excess of stannous chloride should be used according to the added pertechnetate activity and (2) the amount of stannous chloride should be kept as low as possible in order to avoid further reduction of pertechnetate to a lower oxidation state. Moreover, the level of tin impurity in the radiopharmaceutical should be kept as low as possible (DESCRITOFORO, 2007).

The products of the pertechnetate reduction depend on the strength of the reducing agent, the affinity of the available complexing groups and its concentration. Since hydroxide and water have high affinity for reduced technetium and compete with other complexing groups, the reaction's products are greatly influenced by pH (RHODES, 1974; BANERJEE, 2001; MAHAMOOD, 2003). In any case, pertechnetate is a weak oxidant, in acid medium, and it is reduced by weak reductants. Sometimes, an excess of ligand may also act as reducing agent (SAHA, 2004a).

There is a possibility that reduced $^{99m}$Tc may undergo hydrolysis in aqueous solution. In this case, reduced $^{99m}$Tc reacts with water to form various hydrolyzed species depending on the pH, duration of hydrolysis and presence of other agents. An analysis of chemical reaction shows that hydrolysed technetium is a compound of $^{99m}TcO_2$ complexed with other ingredients (e.g., stannous oxide, molybdenum trioxide or aluminum). This hydrolysis competes with the chelation process of the desired compound and thus reduces the yield of $^{99m}$Tc-radiopharmaceutical (SAHA 2004a). The use of stannous chloride has a disadvantage due to the $Sn^{2+}$ ion also readily undergoes hydrolysis in aqueous solution and forms insoluble colloids. These colloids bind to reduced $^{99m}$Tc and thus compromise the labeling yield (SAHA, 2004a).

Besides the stannous chloride method for albumin radiolabeling, the use of ascorbic acid and iron chloride for the labeling of HSA with $^{99m}$Tc was suggested by Harper and the method was developed by Stern, Zolle and McAfee. This method was based on pH changes along the process, what difficult its reproducibility (RHODES, 1974).

### 1.5.4 Quality Control

Radiopharmaceuticals must comply with both radiation and pharmaceutical standard, in order to ensure their safe and efficacious use. The *in vivo* behavior of the radiopharmaceutical is dependent upon its quality, which demands high standards of

radionuclide, radiochemical and chemical purity or particle sizing concerning suspensions. Injections must satisfy additional standards for sterility, apyrogenicity and free from foreign particulate matter (I.A.E.A, 2006). The quality control tests fall into two categories: physicochemical tests and biological tests. The physicochemical tests indicate the level of the radionuclide and radiochemical impurities and determine the pH, ionic strength, osmolality, and physical state of the sample. The biological tests establish the sterility, apyrogenicity and toxicity of the material (SAHA, 2004c).

All radiopharmaceuticals should have an appropriate hydrogen ion concentration or pH value for their stability and integrity. Thus, any deviation from the desired pH must be considered with caution and should be solved (SAHA, 2004c).

The radiochemical purity of a radiopharmaceutical is the fraction of the total radioactivity in the desired chemical form. Radiochemical impurities arise from decomposition due to the action of solvent, change in temperature or pH, light, presence of oxidizing or reducing agents, and radiolysis (SAHA, 2004c). Examples of $^{99m}$Tc radiochemical impurity in $^{99m}$Tc-labeled complexes are $^{99m}TcO_4^-$ and reduced-hydrolyzed $^{99m}$Tc ($^{99m}$Tc-RH). The presence of radiochemical impurities in a radiopharmaceutical results in poor-quality images due to the high background from the surrounding tissues and the blood, and provides unnecessary radiation dose to the patient. To overcome these limitations the radiochemical purity should be superior to 90 % (SAHA, 2004c).

To evaluate the radiochemical purity of a complex, there are many separation techniques, but the rapid radiochemical separations (procedures that can take seconds to minutes) are the most used since many interesting radionuclides used in nuclear medicine studies have short half-lives. To determine the radiochemical purity, of technetium radiopharmaceuticals, ascendant instant thin-layer chromatography or paper chromatography are the most used techniques (MAHER, 2004). Radiochemical impurities are detected using a two-step process: firstly, radiochemical species are separated based on differences in chemical characteristics, and secondly the radioactivity associated with each chemical species is assayed using an appropriate radiation measuring device (I.A.E.A., 2006; ELSINGA, 2010).

During the chromatographic process, different components of the sample distribute themselves between the adsorbent stationary phase and the mobile phase (solvent), depending on their distribution coefficients ($R_f$). Electrostatic forces of the stationary phase tend to retard various components, while the mobile phase carries them along. This effect and the varying solubilities of the different components in the mobile phase cause the individual components to move at different speeds and to appear at different distances along

the paper or ITLC strip. The polarity of the solvent also affects the chromatographic separation of components in a sample. In paper chromatography or ITLC, each component in a given sample is characterized by an $R_f$ value, which is defined as the ratio of the distance traveled by the component has advanced from the original point of application of the test material to the distance of the solvent front (usually $R_f$ value is represented in a scale between 0 to 1) (SAHA, 2004c; DESCRITOFORO, 2007).

It should be noted that radiochemical purity may not be constant, but may change owing to radiolytic decomposition, oxidation-reduction reactions, and interaction with contaminants or stopper/container components, among other factors (ELSINGA, 2010).

# 2. Aim

This thesis aimed the biodistribution study of BSA-NP by nuclear medicine techniques. Therefore, the following aims were defined:

- Optimization of BSA-NP radiolabeling with $^{99m}$Tc;
- Optimization of $^{99m}$Tc-BSA-NP quality control by ascendant micro-cromathography;
- Study the biodistribution of $^{99m}$Tc-BSA-NP, based on a comparative study between $^{99m}$Tc-BSA-NP and $^{99m}$Tc-BSA biodistribution.

# 3. Material and Methods

To improve NP formulation one of the critical points was their behavior *in vivo* and the nuclear medicine was a possible approach to study biodistribution. To apply this imaging technique it was necessary to add a radionuclide to the object of study, in this case the NP. As the BSA was the most external coating, the labelling of BSA with $^{99m}$Tc was the first approach. The radiolabeling method to obtain $^{99m}$Tc-BSA with high radiochemical purity was optimized.

## 3.1 Materials

### 3.1.1 NP production

Low viscosity sodium alginate (viscosity of 1% solution at 25°C, 4-12 cps), dextran sulfate, dextran sulfate, Span® 80, the lipofilic emulsive agent (sorbitan monooleate, HBL = 4.3) and BSA were provided from Sigma-Aldrich (Steinheim, Germany). Micronized calcium carbonate (Setacarb®; 97% of particles with less than 2 µm) was supplied by Omya (Orgon, France). Liquid paraffin (viscosity = 190 mPa.s) was provided by Scharlau (Spain). Human insulin, with recombinant origin and quick action (Actrapid® 100UI/mL) was obtained from Novo Nordisk A/S (Bagsvaerd, Denmark). Desionized water required in the preparation of the solutions was obtained from a Millipore Elix 5 system (Bedford, MA, EUA). The other reagents used were analytical grade.

### 3.1.2 Quality control

ACD (acid citrate-dextrose) was prepared by dissolving 11.3 g of sodium citrate dehydrated ($Na_3C_6H_5O_7 \cdot 2H_2O$), 4.0 g of citric acid monohydrate [$C(OH)(COOH)(CH_2 \cdot COOH)_2 \cdot H_2O$], and 11.0 g of D-glucose ($C_6H_{12}O_6$) in a final volume of 0.5 L of distilled water and sterilized by autoclaving. Acetone and methanol were purchased from Sgima Aldrich®.

The Whatmann No.1 strips and Whatmann 31 ET strips were provided from Whatmann Chromatography Products; the aluminum SG 60 strips (Art. 5553 DC-Alufolien Kieselgel 60) were supplied by MERCK®; finally the aluminum oxide IB-F strips were obtained from J.T. BAKER®. ITLC-SG was supplied by ITLC-SG, Pall Corporation.

### 3.1.3 BSA radiolabeling

The pH was measured by pH-Fix 0-6.0, Machenerey-Nagel. Stannous chloride was used in this formula $Sn_2Cl{\cdot}2H_20$, which was purchased by Aldrich®, it was dissolved in purged ultra-pure water with Argon gas atmosphere and in HCl. The ascorbic acid ($C_6H_6O_6$) from the Sigma® was used in and it was dissolved in ultra-pure water purged with Argon gas atmosphere. The sodium thiosulfate was used in crystal form and it was obtained from Sigma Aldrich®. It was dissolved in ultra-pure water to the concentration mentioned above. The phosphate buffer consists in $Na_2HPO_4{\cdot}2H_2O$ (3.2mmol) from Merck® and $NaH_2PO_4$ (1.0 mmol) Merck® dissolved in 50 ml of ultra-pure water.

The BSA was quantified with Coomassie® Protein Assay Reagent Kit.

NP size was measured with a Coulter LS130 (Beckman Coulter Inc., Fullerton, CA, USA) that has a sensibility between 0.1 and 1000µm.

### 2.1.4 In vivo studies

Mice were received from Laboratories Charles River, Inc. and were maintained in appropriate and acclimatized room, submitted a cycles of 12 hours of light and with free accesses to food (Mucedola 4RFN) and filtered water.

## 3.2 NP production

The NP used in this work have been developed in other projects carried out with the supervision of Professor António Ribeiro *et. al.* (SARMENTO, *et. al.*, 2007a; SARMENTO, *et. al.*, 2007b; WOITISKI, *et. al.*, 2009a; WOITISKI, *et. al.*, 2009b). Thus, the method used to produce NP will be briefly described.

NP were prepared by the emulsification/internal gelation method. The oil phase used was paraffin oil and the emulsifier agent was sorbitan monooleate. The aqueous phase was constituted by alginate, insulin, poloxamer 188, dextran sulfate and calcium carbonate. The emulsion was obtained mixing both phases with marine impellers stirrers, and to promote the obtainment of nanodroplets, the emulsion was sonicated. Acetic acid was added to the emulsion with paraffin oil drop by drop to trigger the internal gelation of alginate and the conditions of stirring and sonication were maintained.

The recuperation of NP scattered in the W/O emulsion was performed by washing with a buffer solution and hexane with an orbital stirring. The separation of the two phases was made in a separating funnel through the addition of propanol and ethanol, maintaining the pH of 4.5. Then, the organic solvents were eliminated by rotary evaporator and the obtained dispersion was sonicated and coated with chitosan followed by the coating with albumin (1% (w/v) at pH 5.1). Finally the pH was adjusted to 5.1.

## 3.2 Quality control

Ascendant micro-chromatography is a method often used to determine radiochemical purity of technetium-99m radiopharmaceuticals and it allows the molecular and physical separation of composts of a sample (SAHA, 2004a). To determine radiochemical purity of $^{99m}$Tc-BSA it was necessary to optimize an appropriate quality control.

### 3.2.1 $^{99m}$Tc-BSA radiochemical purity optimization

For ascendant micro-chromatography, a small aliquot of the radiopharmaceutical preparation was spotted on a paper strip or on an instant thin-layer chromatography (ITLC) strip, which are made of glass fiber impregnated with silica gel (SG) or polysilicic acid (SA), for example. Chromatography was carried out by dipping the spotted strip into an appropriate solvent contained in a chamber, in such a way that the spot remained above the solvent (SAHA, 2004a)

Thereby, two systems were used to allow the quantification of the three possible radiochemical species present in the sample.

First system allowed isolation of free sodium pertechnetate ($^{99m}TcO_4^-$) whose the mobile phase was sodium chloride 0.9 % and solid phase was a strip with 10 cm length and 1 cm

width of instant thin layer cromatography silca gel (ITLC-SG). The strips were marked with fine pencil lines at 1cm ($R_f$=0), 4.5 cm ($R_f$=0.5) and 8 cm ($R_f$=1) from the bottom, as shown in figure 9. This system has been used in nuclear medicine to evaluate many radiopharmaceuticals due to the hydrophilic characteristics of $^{99m}TcO_4^-$ which allow this radiochemical specie go to the top of the strip with the solvent while the other species stay in the bottom (SAHA, 2004c).

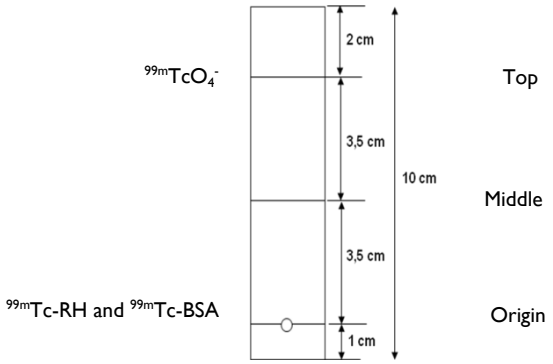


Figure 9 – Scheme of the strip used in the first system.

The second system was tested to separate $^{99m}$Tc-RH from the pretended radiochemical specie, $^{99m}$Tc-BSA. The tested systems were defined taking into account the methods suggested in the bibliography to the $^{99m}$Tc-HSA and aiming the $^{99m}$Tc-RH quantification, and they are presented in the table I (ZOLLE, *et. al.*, 1973; RHODES, 1974; SAHA, 2004c; OZGUR, *et. al.* 2011).

Table 1 – Systems tested to optimize the determination of radiochemical purity (ZOLLE, *et. al.*, 1973; RHODES, 1974; SAHA, 2004c; OZGUR, *et. al.*, 2011)

| | Mobile Phase | Stationary Phase | Strip size (cm) | Method |
|---|---|---|---|---|
| System A | ACD[1] | Aluminum SG[2] 60 | 10 | Paper chromatography |
| System B | ACD | Aluminum Oxide IB-F | 10 | Paper chromatography |
| System C | ACD | ITLC[3]-SG | 10 | ITLC |
| System D | ACD | ITLC-SG | 25 | ITLC |
| System E | ACD | Whatmman 31 ET | 10 | Paper chromatography |
| System F | Methanol 85% | Whatmman No.1 | 10 | Paper chromatography |
| System G | Acetone | Whatmman No.1 | 10 | Paper chromatography |

[1]ACD – Acid citrate-dextrose; [2]SG – Silica gel; [3]ITLC - Instant thin-layer chromatography.

The strips with 25 cm long were marked with fine pencil lines at 2 cm ($R_f$=0), 13.5 cm ($R_f$=0.5) and 24 cm ($R_f$=1) from the bottom of the strip, as shown in figure 10. The strips with 10 cm were marked as the strips used in the first system for all stationary phase tested.

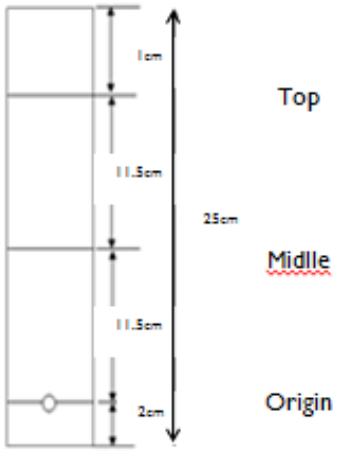


Figure 5 – Scheme of the strips with 25 cm used in the second system.

In general, to carry out the chromatography, an aliquot of radiopharmaceutical was placed at the origin of the strip. Then, it was placed in the chromatographic chamber previously saturated with the solvent for 15min in such a way that the solvent did not contact with the radiopharmaceutical sample. When the solvent achieved the top of the strip, this was taken off the chamber and dried at room temperature. To evaluate the distribution of each radiochemical impurity, this protocol was done with samples of $Na^{99m}TcO_4^-$ and $^{99m}$Tc-RH, separately. The sample of $^{99m}$Tc-RH was obtained mixing $Na^{99m}TcO_4^-$ with 1.11M of stannous chloride, freshly prepared.

The quantification of each specie present on the strip was done by image acquisition to the strip with a camera-gamma and the following parameters, 128x128 matrix, 30 seconds of acquisition, zoom of 1 and an energy peak of 140keV with an energy window of 15%. The images processing was done by marking two regions of interest (ROIs) for each image that correspond to two parts of the strip ($R_f$=0 until $R_f$=0.5 and $R_f$=0 until $R_f$=1).

The percentage of each component was calculated by the ratio between the counts of the isolated component and the total counts of the strip as represented in the equation 1.

$$\%\ ^{99m}TcO_4^- = \frac{Counts_{Rf=0.5\ to\ Rf=1\ of\ the\ first\ system}}{Total\ counts_{strip\ of\ the\ first\ system}} \times 100 \qquad \text{Eq.1}$$

Where,

- $^{99m}TcO_4^-$ is free pertechnetate;
- Counts $R_f$=0.5 to $R_f$=1 of the first system is obtained by the ROI drawn between $R_f$=0.5 to $R_f$=1 in the strip of the first system;
- Total counts strip of the first system is obtained by the ROI drawn in whole strip of the first system.

The radiochemical purity in percentage of $^{99m}$Tc-BSA and $^{99m}$Tc-BSA-NP was calculated by the equation 2.

$$\%\ \text{Radiochemical purity} = 100 - (\%\ ^{99m}TcO_4^- + \%\ ^{99m}\text{Tc-RH}) \qquad \text{Eq. 2}$$

Where,

- $^{99m}TcO_4^-$ is free pertechnetate;
- $^{99m}$Tc-RH is technetium reduced-hydrolyzed.

The radiochemical purity of $^{99m}$Tc-BSA complex was measured at 5, 15, 60, 120, 360, 720 and 1440 minutes after the radiolabeling procedure. Concerning $^{99m}$Tc-BSA-NP, the

radiochemical purity was measured after each step, namely, coating, pH adjustment, centrifugation and sonication, which were carried out 45, 50, 60 and 75 minutes after the radiolabeling $^{99m}$Tc-BSA, respectively. Furthermore, $^{99m}$Tc-BSA-NP radiochemical purity was also measured at 120, 360, 720 and 1440 minutes after the radiolabeling of $^{99m}$Tc-BSA.

## 3.3 BSA radiolabelling optimization

In order to optimize the radiolabeling method used to achieve the labeled BSA with $^{99m}$Tc several conditions were tested, namely, albumin mass, the reducing agent and its concentration, ascorbic acid concentration, volumetric activity of $Na^{99m}TcO_4^-$, pH, temperature, stirring and incubation time.

The pH was evaluated by color comparison method.

The albumin tested was the same used in the NP coating and for this reason the concentration and pH of the solution were the same. Nevertheless, three quantity of albumin was tested, 1, 2 and 5mg.

In this work the stannous chloride dihydrated was dissolved in purged ultra-pure water with Argon gas atmosphere and in HCl, at different concentrations, as indicated in table 2 e 3. The radiolabeling procedures presented in table 1 and 2 were carried out by adding each compound in the following sequence: stannous chloride, BSA and $Na^{99m}TcO_4^-$, after this the vial was manually shaken and incubated at room temperature. All vials used in these procedures were purged with Argon gas atmosphere before it was used.

Table 2 – Conditions tested with stannous chloride dissolved in water and in HCl (RHODES, 1974; WANG, *et. al.*, 2011).

| | Stannous chloride (µl) | Stannous chloride (mmol) | BSA[1] (mg) | $Na^{99m}TcO_4^-$ [2] (MBq/ml) | Protocol |
|---|---|---|---|---|---|
| Stannous chloride dissolved in water | 200 | $8.86x10^{-4}$ | 1 | 592 | A |
| | | | | 1110 | B |
| | | | 2 | 592 | C |
| | | | | 1110 | D |
| Stannous chloride dissolved in HCL | 10 | 10 | $0.44x10^{-4}$ | 93 | E |

[1]BSA – Bovine serum albumin; [2]$Na^{99m}TcO_4^-$ - Sodium pertechnetate

The adding of ascorbic acid was carried out to improve the radiolabeling efficiency. It was added after the stannous chloride, following the sequence above mentioned in the table 3.

Table 3 - Conditions tested with stannous chloride and ascorbic acid dissolved in water (ZOLLE, *et. al.*, 1973; RHODES, 1974; YOKOYAMA, *et. al.*, 1975).

| | Stannous chloride | | Ascorbic Acid | | BSA[1] | $^{99m}TcO_4^-$ [2] | Protocol |
|---|---|---|---|---|---|---|---|
| | µl | mmol | µl | Mmol | mg | MBq/ml | |
| Stannous chloride dissolved in water | 400 | $1.8x10^{-3}$ | 500 | $2.8x10^{-3}$ | 1 | 111 | F |
| | | | | | | 296 | G |
| | | | | | | 592 | H |
| | | | | | 5 | 111 | I |
| | | | | | | 296 | J |
| | | | 500 | $14.2x10^{-3}$ | 1 | 111 | K |
| | | | | | 5 | 111 | L |
| | | | | | | 296 | M |

[1]BSA – Bovine serum albumin; [2]$Na^{99m}TcO_4^-$ - Sodium pertechnetate

Nevertheless, the influence of temperature was tested in protocol N, heating at 40°C for ten minutes follow the protocol J procedure.

The pH influence was tested with the composition of protocol J. It was carried out with a decreasing of pH to 2 before the addition of $Na^{99m}TcO_4^-$ as it also had a pH of 2 (protocol O). This protocol was repeated with pH values of 1 (protocol P).

Thus, other method to radiolabeling BSA with $Na^{99m}TcO_4^-$ was carried out. It consists in a mixture of sodium thiosulfate 10 $mg.ml^{-1}$; HCl, N; and 1110 to 2220 MBq of $Na^{99m}TcO_4^-$ (1.0/1.0/0.5) (v/v/v) that is heated at 100°C for 3.5 minutes with a dry bath. At the end of this time the vial was cooled in running water for 5 minutes to low the temperature to room temperature. Then, 2.5 ml of BSA was added and the vial was stirring with vortex for 30 seconds. Finally, 2 ml of pH 7.4 phosphate buffer was added and the vial was manually shaken (PAOLI ,*et. al.*, 1966; CRAGIN, 1969).

### 3.3.1 NP radiolabeling

In respect to the radiolabeling of the NP, these were coated with the $^{99m}$Tc-BSA in spite of radiolabeling the BSA after incorporating in the NP. To coat NP the pH of $^{99m}$Tc-BSA was adjusted to 5.1 (15 minutes after the radiolabeling) and the procedure was performed with the same conditions used to coat the NP with BSA. At this point the NP were centrifuged at 56 *g* for 5 minutes; these conditions were optimized with tests made to eliminate the BSA that did not interact with the NP, as described below. Following, the NP were sonicated (A=50 KHz) for 10 minutes.

#### 3.3.1.1 Optimization of the parameters to the centrifugation

To evaluate the best condition to centrifuge NP and eliminate the unloaded BSA, different conditions were tested and the quantification of BSA present in the supernatant was performed with Coomassie® Protein Assay Reagent Kit. The test was executed with insulin-free NP since the kit reacts with proteins indiscriminately. The conditions tested were the following: (1) 5585 *g* for 10 min; (2) 1396 *g* for 10 min; (3) 56 *g* for 10min; (4) 56 *g* for 5min. The protocol for the quantification allowed a working range from 1 µg to 25 µg of BSA and it consisted in mixing 5 µl of the sample with 250 µl of the Coomassie Reagent and incubate for 10 min at room temperature; the absorbance was measured at 595 nm and the average reading for the blank replicates was subtracted from the samples replicates. All measurements were performed in triplicate. To determine the protein concentration of each sample, a standard curve was prepared by plotting the average blank-corrected 595 nm reading for each BSA standard concentration in µg/mL.

### 3.3.2 NP characterization

To ensure similarity between NP and $^{99m}$Tc-BSA-NP, a study to compare these NP relatively to their size and zeta potential was designed. Thus, the procedure done to radiolabel BSA and to coat the NP was carried out with an eluate 8 days old. Thereby, BSA was labelled with $^{99}$Tc and, since the dose calibrator does not have sensibility to measure such a low activity, the activity of $^{99m}$Tc present in the sample was calculated theoretically by the equation 3.

$$A = A_0 e^{-\lambda t} \qquad \text{Eq. 3}$$

Where,

- A is the acivity (MBq),
- $A_0$ is the initial activity (MBq),
- e is the base of the natural logarithm,
- λ is the decay constant, and
- t the time in days.

$$A = 925e^{-2.772 \times 8} \text{ MBq}$$
$$A = 2.16 \times 10^{-7} \text{ MBq}$$

The NP and the $^{99}$Tc-BSA-NP size was detected, both from the same batch, by laser diffraction. The measurements were done in triplicate.

## 3.3 *In vivo* studies

The purpose of the *in vivo* studies was determining the behavior of the NP in their local of administration and its biodistribution, with particular attention to the gastrointestinal tract. A comparative study between $^{99m}$Tc-BSA-NP and $^{99m}$Tc-BSA was carried out through the oral administration of both radiopharmaceuticals to characterize the remaining time in the gastrointestinal tract, the adhesion to the intestinal wall and the absorption to the bloodstream. The radiopharmaceutical was administrated by gavage as represented in figure 11. The studied animals were maintained with its habitual food and water and they were not sedated in order ensure the physiologic gastrointestinal transit.

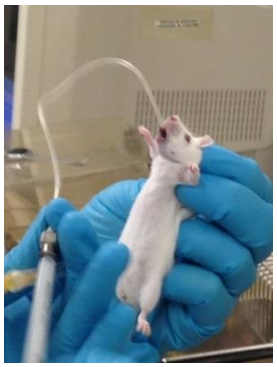

Figure 6 – Gavage administration

An image in posterior projection was acquired and the animals were killed by cervical dislocation, according to the legislation, at 0, 30, 60, 90, 120, 180, 360 and 1440 minutes after the administration. At this time the gastrointestinal tract, the thyroid, the lungs, the liver, muscle, the kidneys and blood were collected and an image was acquired. The gastrointestinal tract was divided in order to individualize the stomach, the duodenum, the small intestine (jejunum and ileum) and the large intestine. For each portion the content was separated from the wall and placed in an individual container. All the portions of the wall were individually washed in running water in an appropriate washstand to the procedure, and placed in an individual container. Images were acquired from each gastrointestinal content and from the wall and their mass (mg) was obtained, as well as, the mass (mg) of all organs and fluids collected. All the images were acquired with a gamma-camera (GE 400 AC) collimated for a low energy high resolution (LEHR) collimator and controlled by an acquisition computer Genie Acq. All the images were acquired with the same parameters, namely, 256x256 matrix, 2 minutes of acquisition, zoom of 2 and an energy peak of 140keV with an energy window of 15%. The images were transferred to the Xeleris work station to be processed. The image processing consisted of the calculation of the total counts of the ROI drawn in each mouse image after the radiopharmaceuticals administration over the organs, the fluids, the gastrointestinal content and the walls to obtain activity/time curves, and to calculate the percent of the activity administered per mass unit (%AA/mg) according to equation 4.

$$\%\ Activity\ administered/mg = \frac{Total\ Counts/mg}{Counts\ of\ activity\ administered} \times 100 \qquad \text{Eq. 4}$$

Where,

- Total counts is value obtained for the ROI drawn in the images of each organ, fluid, GI content or GI walls;
- mg is the weight of each organ, fluid, GI content or GI walls
- Counts of activity administered is counts obtained in the ROI drawn in the image

The animal killed 24 hours after the administration, was placed in an individual cage with a known weight which image was acquired at the same time of the sacrifice. These images were acquired with the same parameters of acquisition used to the other images acquired in the *in vivo* studies and the processing done was the same, as well.

# 4. Results

According to the methods previously described this chapter presents the results obtained concerning the radiolabeling of $^{99m}$Tc-BSA, its quality control, and the biodistribution of $^{99m}$Tc-BSA-NP using Balb/c mice comparing to the biodistribution of $^{99m}$Tc-BSA.

## 4.1 Quality Control

First the quality control was optimized in order to evaluate the radiochemical purity. The ascendant micro-chromatography allows separate the different radiochemical species according to the chromatographic system used. The results to the different systems tested are present in table 4.

Table 4 – The $^{99m}TcO_4^-$ and $^{99m}$Tc-RH Rf for each system tested. Composition of each system was previously described in table 1, page 37.

| System | $^{99m}TcO_4^-$ ($R_f$[1]) | $^{99m}$Tc-RH ($R_f$) |
|---|---|---|
| A | 0.0 | 0-1 |
| B | 0.5-1.0 | 0.0 |
| C | 1.0 | 0-1 |
| D | 1.0 | 0.5-1.0 |
| E | 0.5 | 0-1.0 |
| F | 0.5 | 0.0 |
| G | 1.0 | 0.0 |

[1] $R_f$ – distribution coefficient

The chromatographic systems tested aimed to isolate the $^{99m}TcO_4^-$ and the $^{99m}$Tc-RH from the $^{99m}$Tc-BSA, in order to calculate de labeling efficiency of the $^{99m}$Tc-BSA complex.

According to table 4, for the seven systems tested, the systems C, D and G present a high affinity to $^{99m}TcO_4^-$. This affinity is lower in the system B since, the mobile phase does not carry the whole of $^{99m}TcO_4^-$ to the top of the strip. The systems E and F show some affinity to $^{99m}TcO_4^-$ but only the middle of the strip was achieved. System B, F and G do not have affinity towards $^{99m}$Tc-RH that is higher in the systems A, C and G, although it is insufficient to carry the whole of this radiochemical specie to the top of the strip.

Since, the $^{99m}$Tc-BSA presents $R_f$ equals to zero, which is due to its high molecular weight the system D has the best performance, because it allow separating radiochemical impurities from the radiochemical pretended specie and calculate the radiochemical purity of the radiopharmaceutical. Thus, the percentage of radiochemical impurities in the sample was calculated according to the following equation (equation 5).

$$\% \, ^{99m}\mathrm{Tc-RH} + {}^{99m}\mathrm{TcO4}^- = \frac{Counts_{Rf=0.5 \; to \; Rf=1 \; of \; the \; second \; system}}{Counts_{total \; strip \; of \; the \; second \; system}} \times 100 \qquad \text{Eq. 5}$$

Where,

- $^{99m}$Tc-RH is technetium reduced-hydrolyzed;
- $^{99m}TcO_4^-$ is free sodium pertechnetate;
- Counts $R_f$=0.5 to $R_f$=1 of the second system (system D) is obtained by the ROI drawn between $R_f$=0.5 to $R_f$=1 in the strip of the second system;
- Counts strip of the second system is obtained by the ROI drawn in whole strip of the second system.

## 4.2 Radiochemical purity of $^{99m}$Tc-BSA

With the aim of optimizing the radiolabeling of BSA with $Na^{99m}TcO_4^-$ different protocols were tested as described in chapter 3. Experimental conditions tested were pH, reducing agents, concentration of the kit components, labelling temperature. The radiochemical purity obtained for each protocol is displayed in table 5.

Table 5 – Results obtained to the different radiolabeling protocols tested (n=1). The radiochemical purity (percentage) excludes the percentage of $^{99m}TcO^{4-}$ and $^{99m}$Tc-RH present in each sample. Composition of each system was previously described in tables 2 and 3, page 40.

| Protocol | Radiochemical Purity (%) | Time after radiolabeling (minutes) | Time of stability (minutes) | pH |
|---|---|---|---|---|
| A | 92.0 | 30 | <30 | 6 |
| B | 89.7 | 30 | <30 | 6 |
| C | 93.7 | 30 | <30 | 6 |
| D | 94.1 | 30 | <30 | 6 |
| E | 28.2 | 30 | 30 | 3 |
| F | 70.3 | 300 | 240 | 5 |
| G | 82.6 | 120 | 60 | 5 |
| H | 68.8 | 180 | <30 | 5 |
| I | 86.1 | 360 | <30 | 5 |
| J | 22.2 | 30 | 240 | 5 |
| K | 19.9 | 30 | 120 | 4 |
| L | 26.9 | 30 | 360 | 4 |
| M | 23.4 | 30 | 360 | 4 |
| N | 27.1 | 15 | 360 | 5 |
| O | 87.2 | 120 | 60 | 2 |
| P | 32.2 | 30 | 240 | 1 |
| Q | 95.8 | 30 | 360 | 2 |

The results present in the table 5, reveal that the protocols A, C, D and Q have radiochemical purity higher than 90% as it is requested to a radiopharmaceutical for clinical use. However, these formulations have different stability after radiolabeling. As a matter of fact, the protocol Q reveal the best results due to its radiochemical purity higher than 95% achieved 30 minutes after the radiolabeling and high stability over 360 minutes studied. Following the selection of protocol Q, a detailed study in order to evaluate the reproducibility of the results, as well as the influence of pH changes in the stability of the radiochemical purity, was performed. The results are shown in figure 12 and in table 6.

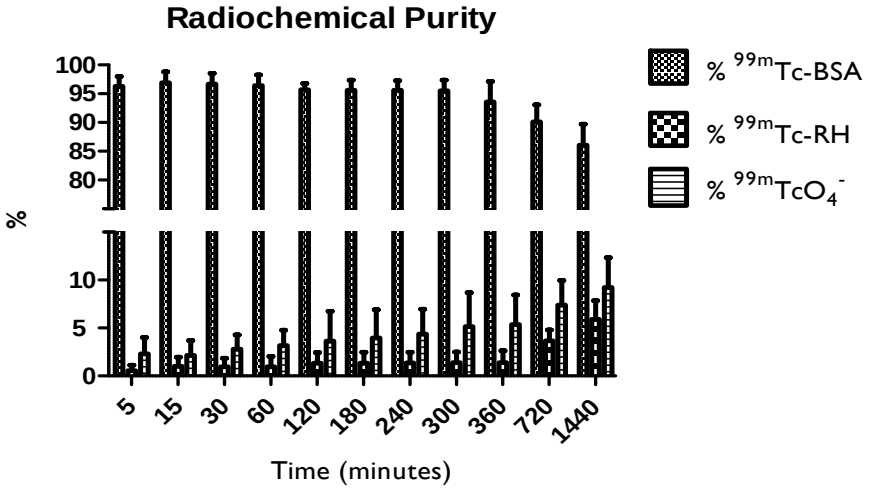


Figure 12 – The percentage of $^{99m}$Tc-BSA, $^{99m}TcO_4^-$ and $^{99m}$Tc-RH obtained with protocol Q (n=6).

The radiochemical purity of $^{99m}$Tc-BSA achieves the maximum value around 96% five minutes after the radiolabeling that is maintained during 300 minutes. At 720 minutes after the radiolabeling the radiochemical purity still higher than 90% and the minimum value occurs at 1440 minutes.

Table 6 - The percentage of $^{99m}$Tc-BSA, $^{99m}TcO_4^-$ and $^{99m}$Tc-RH obtained with protocol Q (n=6).

| Time (minutes) | % $^{99m}$Tc-BSA (mean ± SD[1]) | % $^{99m}$Tc-RH (mean ± SD) | % $^{99m}TcO_4^-$ (mean ± SD) |
|---|---|---|---|
| 5 | 96.29 ±1.69 | 0.56 ±0.56 | 2.31 ±1.71 |
| 15 | 96.90 ±1.90 | 1.00 ±0.95 | 2.16 ±1.54 |
| 30 | 96.67 ±1.85 | 0.97 ±0.89 | 2.79 ±1.48 |
| 60 | 96.44 ±1.84 | 0.95 ±1.08 | 3.18 ±1.58 |
| 120 | 95.70 ±1.09 | 1.34 ±1.12 | 3.64 ±3.12 |
| 180 | 95.63 ±1.74 | 1.35 ±1.13 | 3.95 ±2.96 |
| 240 | 95.59 ±1.68 | 1.37 ±1.11 | 4.37 ±2.58 |
| 300 | 95.52 ±1.85 | 1.40 ±1.10 | 5.15 ±3.54 |
| 360 | 93.56 ±3.57 | 1.41 ±1.24 | 5.36 ±3.09 |
| 720 | 90.10 ±2.99 | 3.66 ±1.14 | 7.39 ±2.58 |
| 1440 | 86.04 ±3.66 | 5.90 ±1.96 | 9.22 ±3.11 |

[1]SD – standard deviation

After BSA labeling with $^{99m}$Tc, the NP coating was optimized to be carried out with a BSA solution at pH 5.1. Since the pH of the $^{99m}$Tc-BSA solution obtained with protocol Q is 2, the increase of pH is required. The influence of pH increase up to 5 is demonstrated in figure 12 and in table 7. The pH was increased 15minutes after the radiolabeling, at least.

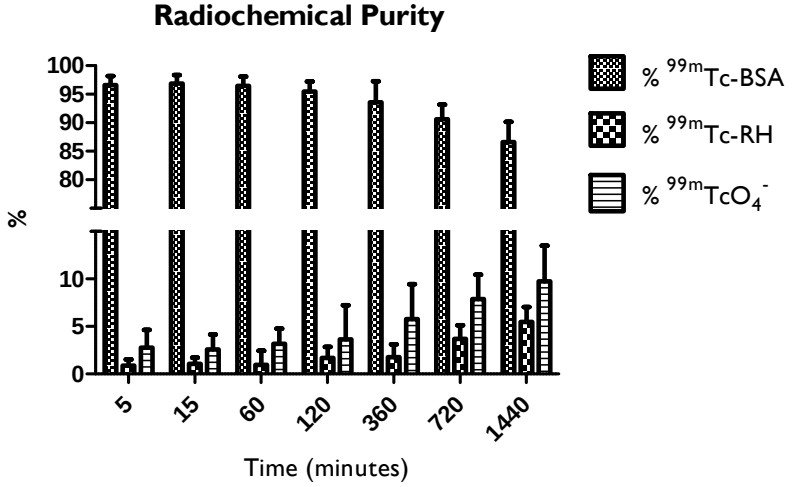


Figure 12 – The percentage of $^{99m}$Tc-BSA, $^{99m}TcO_4^-$ and $^{99m}$Tc-RH obtained with protocol Q and the increase of pH to 5 after 15 minutes (n=8).

Table 7 - The percentage of $^{99m}$Tc-BSA, $^{99m}TcO_4^-$ and $^{99m}$Tc-RH obtained with protocol Q and the increase of pH to 5 after 15 minutes (n=8).

| Time (minutes) | % $^{99m}$Tc-BSA (mean ± SD[1]) | % $^{99m}$Tc-RH (mean ± SD) | % $^{99m}TcO_4^-$ (mean ± SD) |
|---|---|---|---|
| 5 | 96.60 ±1.58 | 0.88 ±0.65 | 2.76 ±1.86 |
| 15 | 96.85 ±1.48 | 1.06 ±0.65 | 2.58 ±1.58 |
| 60 | 96.48 ±1.58 | 0.97 ±1.46 | 3.18 ±1.58 |
| 120 | 95.49 ±1.75 | 1.68 ±1.17 | 3.64 ±3.60 |
| 360 | 95.58 ±3.68 | 1.77 ±1.35 | 5.76 ±3.68 |
| 720 | 90.59 ±2.58 | 3.69 ±1.44 | 7.87 ±2.58 |
| 1440 | 86.60 ±3.58 | 5.50 ±1.57 | 9.73 ±3.77 |

[1]SD – standard deviation

The influence of increasing pH, on the radiochemical purity, can be observed 60 minutes after the radiolabeling. Values still higher than 95 %, around 96 %, so no changes were detected comparing to radiochemical purity at pH 2. Therefore, no influence is observed and radiochemical purity is higher than 90 % even at 720 minutes after the radiolabeling.

## 4.3 NP coating with $^{99m}$Tc-BSA

The NP were coated with $^{99m}$Tc-BSA respecting the coating protocol optimized to these NP. Thus, the quality control done to NP was performed to evaluate if the coating protocol of NP do not affect the radiolabeling efficiency of $^{99m}$Tc-BSA. These results are showed in the figure 13 and in the table 8.

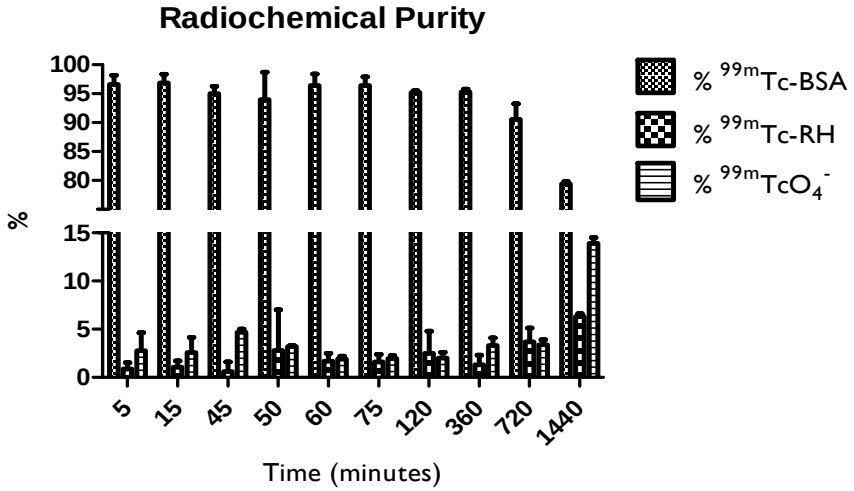


Figure 13 – The percentage of $^{99m}$Tc-BSA, $^{99m}TcO_4^-$ and $^{99m}$Tc-RH obtained with protocol Q and the increase of pH to 5 after 15 minutes. The graphic shows the influence of NP coating protocol with $^{99m}$Tc-BSA after the NP coating at 45minutes, the increase of pH at 50 minutes, the NP centrifugation at 60minutes and the NP sonication at 75minutes after the radiolabeling of $^{99m}$Tc-BSA (n=8).

Table 8 - The percentage of $^{99m}$Tc-BSA, $^{99m}TcO_4^-$ and $^{99m}$Tc-RH obtained with protocol Q and the increase of pH to 5 after 15 minutes. The graphic shows the influence of NP coating protocol with $^{99m}$Tc-BSA after the NP coating at 45minutes, the increase of pH at 50 minutes, the NP centrifugation at 60minutes and the NP sonication at 75minutes after the radiolabeling of $^{99m}$Tc-BSA (n=8).

| Time (minutes) | % $^{99m}$Tc-BSA (mean ± SD) | % $^{99m}$Tc-RH (mean ± SD) | % $^{99m}TcO_4^-$ (mean ± SD) |
|---|---|---|---|
| 5 | 96.60 ±1.58 | 0.88 ±0.65 | 2.76 ±1.86 |
| 15 | 96.85 ±1.48 | 1.06 ±0.65 | 2.58 ±1.58 |
| 45 | 95.00 ±1.30 | 0.60 ±1.00 | 4.70 ±0.30 |
| 50 | 94.00 ±4.70 | 2.80 ±4.20 | 3.20 ±0.10 |
| 60 | 96.40 ±2.00 | 1.70 ±0.80 | 1.90 ±0.30 |
| 75 | 96.40 ±1.50 | 1.60 ±0.80 | 1.97 ±0.30 |
| 120 | 95.20 ±0.30 | 2.50 ±2.30 | 2.00 ±0.60 |
| 360 | 95.30 ±0.50 | 1.30 ±1.00 | 3.30 ±0.80 |
| 720 | 90.58 ±2.97 | 3.69 ±1.44 | 3.40 ±0.50 |
| 1440 | 79.40 ±0.40 | 6.30 ±0.30 | 13.90 ±0.60 |

[1]SD – standard deviation

The $^{99m}$Tc-BSA-NP radiochemical purity is bigger than 95 % until 360 min after the radiolabeling. It presents a slight decrease to 94 % at 50 min after the radiolabeling when the NP pH is increased, however the radiochemical purity returns to values above 96% after the centrifugation (60 min after radiolabeling). The radiochemical purity remains bigger than 90% until 720 min after radiolabeling and the minimum value is only achieved 1440 minutes after the radiolabeling.

After quality control, the influence of coating protocol of NP with $^{99m}$Tc-BSA was also evaluated in respect of NP size as represented in the figure 14. Both $^{99m}$Tc-BSA-NP and BSA-NP shows a median diameter between 194-198 ± 0.04 nm. As it can be seen, $^{99m}$Tc-BSA-NP presents a size distribution curve with more higher-sized particles (d90 % = 1870 ± 1659 nm) than BSA-NP (d90 % = 563 ± 5.6 x $10^{-3}$). However, the curve distribution is slightly altered after BSA-NP radiolabeling.

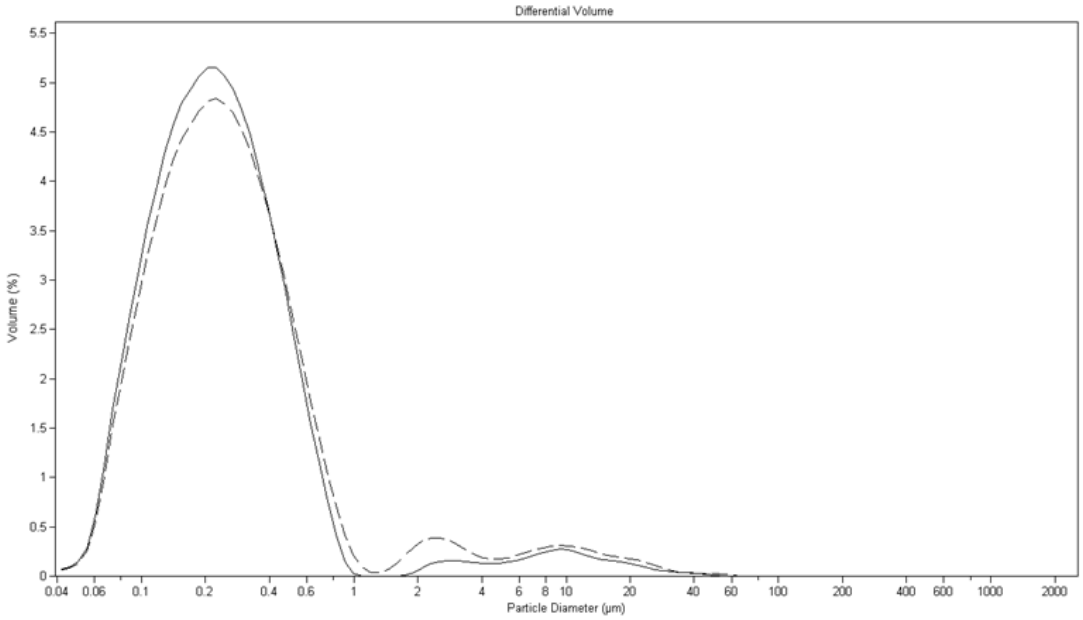


Figure 14 - Representation of the size distribution, where the complete line corresponds to the NP-BSA and the score line corresponds to the $^{99m}$Tc-BSA-NP. The pH increasing, the centrifugation and the sonication were carried out at the same conditions for both.

### 4.3.1 Optimization of the parameters to the centrifugation

After NP coating with $^{99m}$Tc-BSA, it is important to ensure that all the existent activity is only due to the $^{99m}$Tc-BSA present in coated NP. Thus, different centrifugation protocols were optimized, considering the concentration of BSA present in the supernatant after each centrifugation. A calibration curve prepared with BSA standard concentrations in µg/ml was obtained with a $R^2$ equal to 0.98. The results obtained for protein quantification in the supernatant by using the Coomassie® Protein Assay Reagent Kit in function of centrifugation, are described in table 9.

Table 9 – The percentage of BSA present in the supernatant after different after different protocols based on different acceleration and time of centrifugation.

| Protocol | Aceleration (*g*) | Time (minutes) | BSA in supernatant (%) |
|---|---|---|---|
| 1 | 5585 | 10 | 49.22 |
| 2 | 1396 | 10 | 63.50 |
| 3 | 56 | 10 | 65.91 |
| 4 | 56 | 5 | 61.03 |

[1]BSA – bovine serum albumin

It is possible to observe that the protocol 1 (5585g during 10 minutes) concentrates the lowest percentage of BSA in the supernatant, while the three protocols present higher concentrations, and all of them in the same range.

## 4.4 In vivo studies

A comparative study between $^{99m}$Tc-BSA and $^{99m}$Tc-BSA-NP biodistribution was carried out. For each radiopharmaceutical 32 animals were studied. Following oral administration of radiopharmaceuticals to animals, biodistribution was assessed by determination of both radiopharmaceuticals at different times (n=4 for each time studied). The animals chosen were 8-10 week old balb-c male mice, with 22-26g of weight. The activity administered in each animal was on average 15.3 MBq (± 2.6 MBq). Following mice sacrifice the gastrointestinal tract, organs and fluids were collected and images were acquired in the camera-gama.

This chapter shows the obtained results for $^{99m}$Tc-BSA and $^{99m}$Tc-BSA-NP biodistribution, first separately and then making comparisons.

### 4.4.1 Imaging

In the *in vivo* studies the images acquired with camera-gamma were a fundamental tool, due to the quantitative data and qualitative information that they can give. At the mice sacrifice the gastrointestinal tract were collected and an image was acquired before the separation and the cleaning of gastrointestinal contents. The images of the figure 15 and 16 are exemplified for $^{99m}$Tc-BSA and $^{99m}$Tc-BSA-NP, respectively.

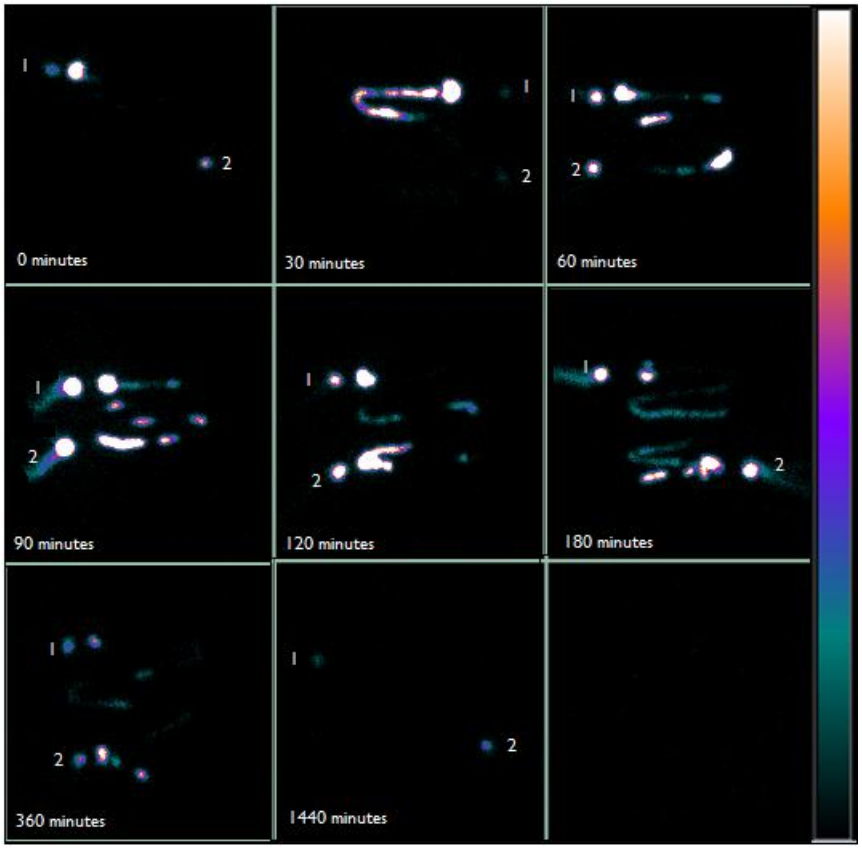


Figure 15 – The gastrointestinal tract images over time, at 0, 30, 60, 90, 120, 180, 360 and 1440 minutes for $^{99m}$Tc-BSA. The number 1 and 2 in each image are anatomical marks, which indicates the stomach and cecum, respectively.

Taking into account the qualitative analyses of the images in depicted figure 17 the progression of the $^{99m}$Tc-BSA in the gastrointestinal tract is observed. No activity is detected at time 0 and 30 minutes after the administration is possible to appreciate the activity in the duodenum and in the initial part of the jejunum. In the next 60 minutes the activity is distributed by whole small intestine, which means that it contains the radiopharmaceutical. At 120 minutes, the activity arrives to the cecum and then after 60 minutes almost all the activity is in the large intestine. The elimination of the radiopharmaceutical of the small intestine is almost complete at 360 minutes after the administration. At 1440 minutes no activity is seen in the gastrointestinal tract.

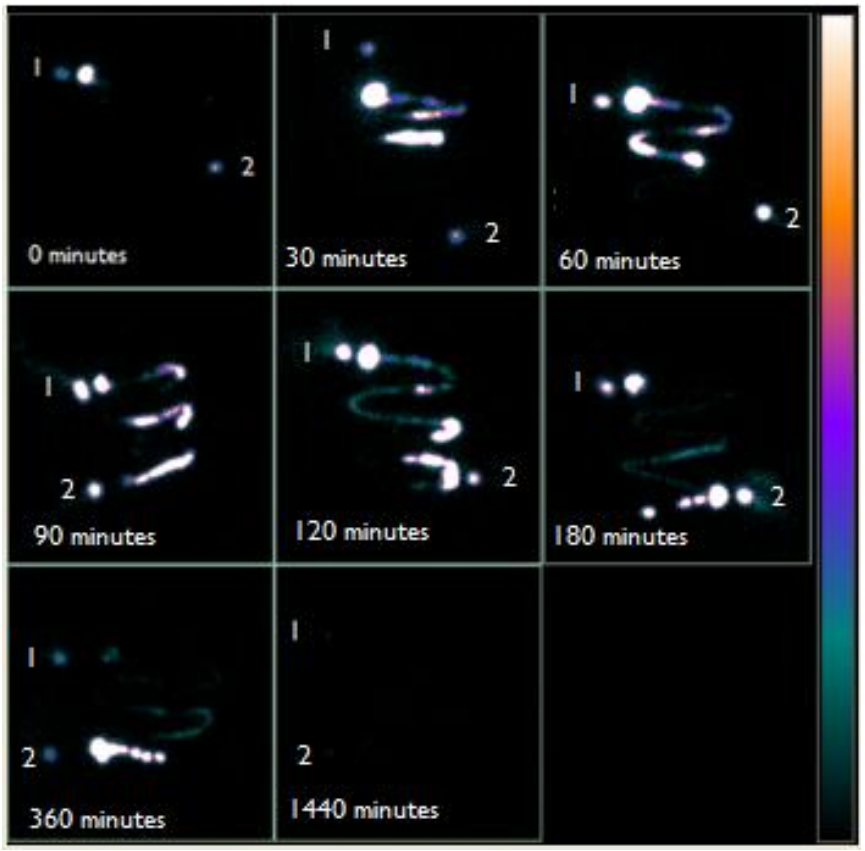


Figure 16 - The gastrointestinal tract images over time, at 0, 30, 60, 90, 120, 180, 360 and 1440 minutes for $^{99m}$Tc-BSA-NP. The number 1 and 2 in each image are an anatomical mark, which indicates the stomach and cecum, respectively.

The qualitative analyze of the images of figure 18, allows monitoring the progression of $^{99m}$Tc-BSA-NP in the gastrointestinal tract. Thirty minutes after the administration is possible to see activity in the duodenum and in the jejunum. In the next 60 minutes the radiopharmaceutical was spread in small intestine. At 120 minutes after the administration, the activity reaches the cecum and followed more 60 minutes almost all the activity is in the large intestine. The progression in the small intestine of the radiopharmaceutical is

maintained until 360 minutes. Lastly, 1440 minutes after the administration no activity is seen in the gastrointestinal tract.

Furthermore, images of organs and fluids collected and the gastrointestinal walls and contents were acquired. The results were obtained through ROIs mapping in these images acquired, as illustrated in the figure 17 and 18.

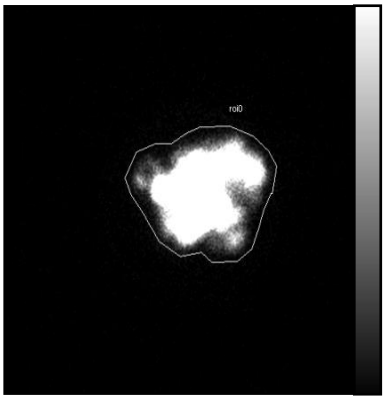


Figure 7 – ROI mapped in an image acquired after the administration

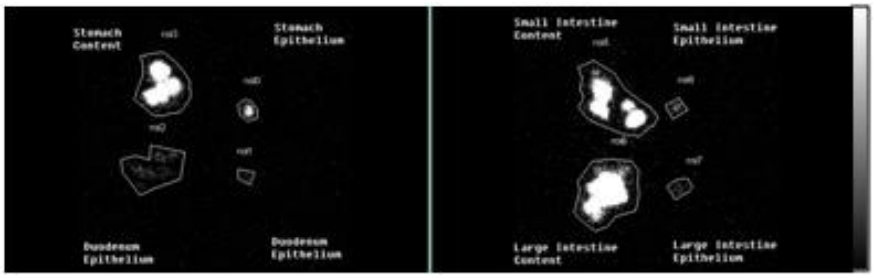


Figure 18 - ROIs drawn in the image corresponding to the contents and walls of the gastrointestinal tract, as indicated in the image.

The qualitative and quantitative analyses of the results are complementary for the understanding of the radiopharmaceuticals biodistribution. The qualitative analyses of the images hardly allow differences between the radiopharmaceuticals. So, these are more perceptible with the quantitative date analyses.

### 4.4.2 Quantitative analyses of $^{99m}$Tc-BSA

Results of $^{99m}$Tc-BSA biodistribution shows its progression in the gastrointestinal tract for 1440 minutes. The percentage of administered activity *per* mg calculated in different organs and fluids studied is shown in the figure 19.

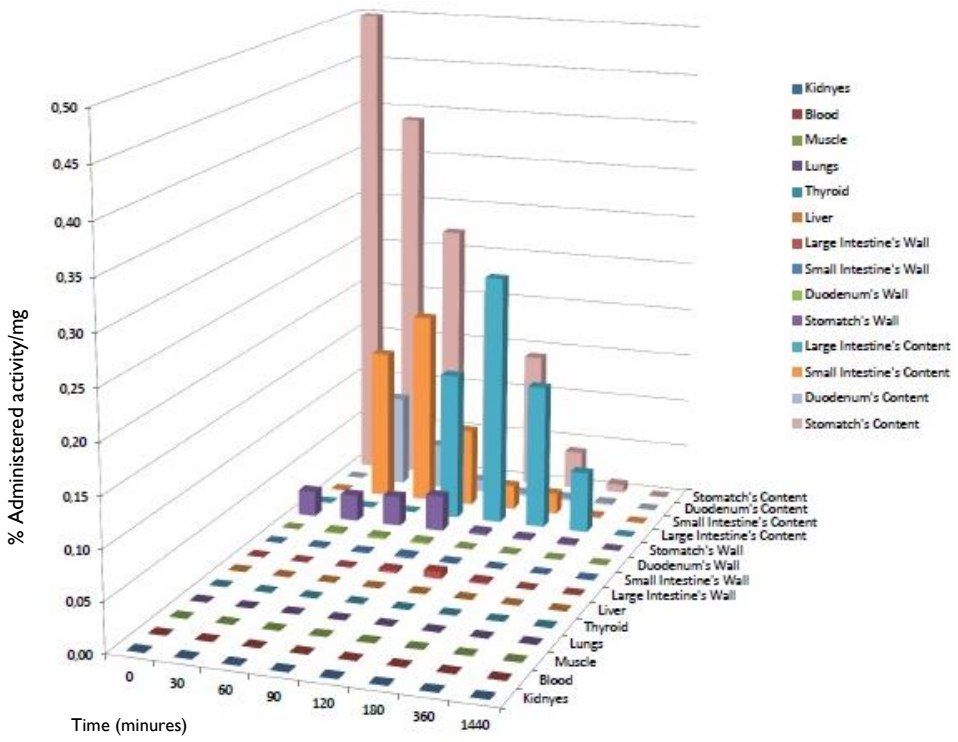


Figure 19 - Biodistribution in percentage administered activity/mg of $^{99m}$Tc-BSA in the gastrointestinal contents, gastrointestinal walls, liver, thyroid, lungs, muscle, blood and kidneys along the time.

The exactly values of activity in different samples represented in figure 19 are in annex 11. The highest percentage of activity *per* mg is found in the stomach's content, because it is the local of administration. The activity present in the organs and fluids beyond gastrointestinal tract is minimal, as well as, the activity present in the gastrointestinal walls showing, however, higher values in the stomach's wall. The activity present in the stomach's content decreases over time showing total elimination only 1440 minutes after the administration, however the activity values after 360 minutes are already residual. The activity duodenum's content reaches a peak 30 minutes after the administration while the peak of activity in the small intestine's content is attained 60 minutes after the administration and the progression shows the lower values at 360 minutes. In the large intestine's content the maximum value occurs 120 minutes after the administration but at 360 minutes a considerable activity is still present. The complete radiopharmaceutical elimination only occurs 1440 minutes after the administration.

The figure 20 displays the percentage of administered activity per mg for each gastrointestinal wall following administration until 360 minutes.

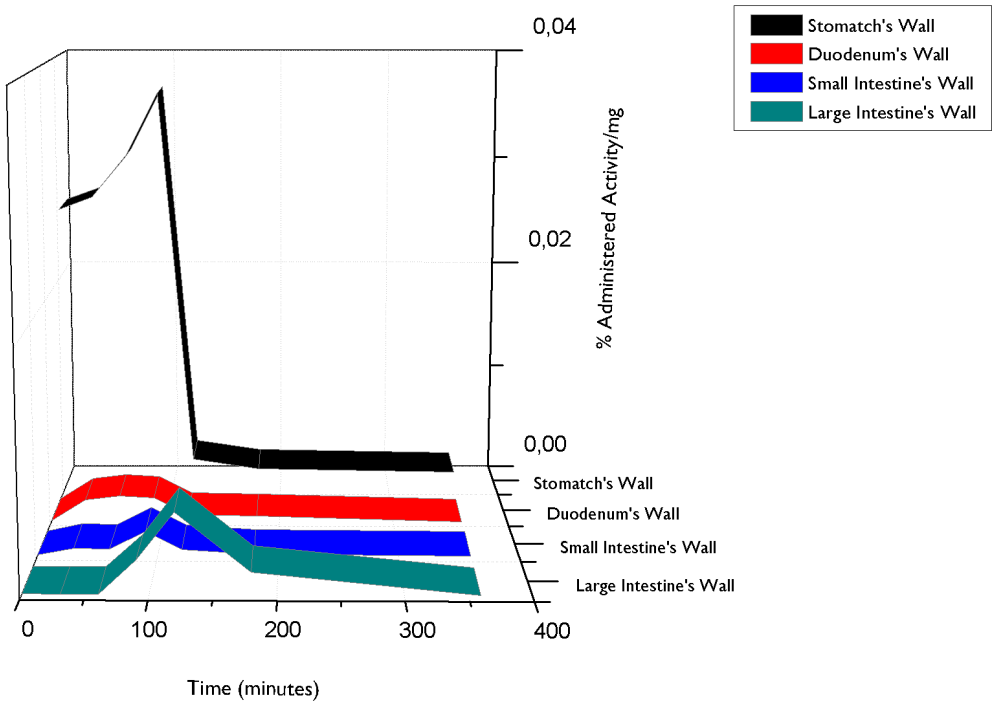


Figure 8 - The percentage administered activity/mg of $^{99m}$Tc-BSA in the gastrointestinal walls.

The activity present in the stomach's wall achieves the maximum value at 90 minutes after the administration with a marked decrease at 120 minutes. The higher activity in the duodenum's wall is attained at 60 minutes after the administration and 360 minutes after the administration there are no activity there. The activity in the small intestine's wall shows a peak at 90 minutes after the administration and at 120 minutes the value of activity returns to the baseline values. The large intestine's wall has a peak of activity 120 minutes after the administration that decreases to the base values at 180 minutes.

The figure 21 shows the percentage of administered activity *per* mg of the each portion of gastrointestinal tract content for 360 minutes.

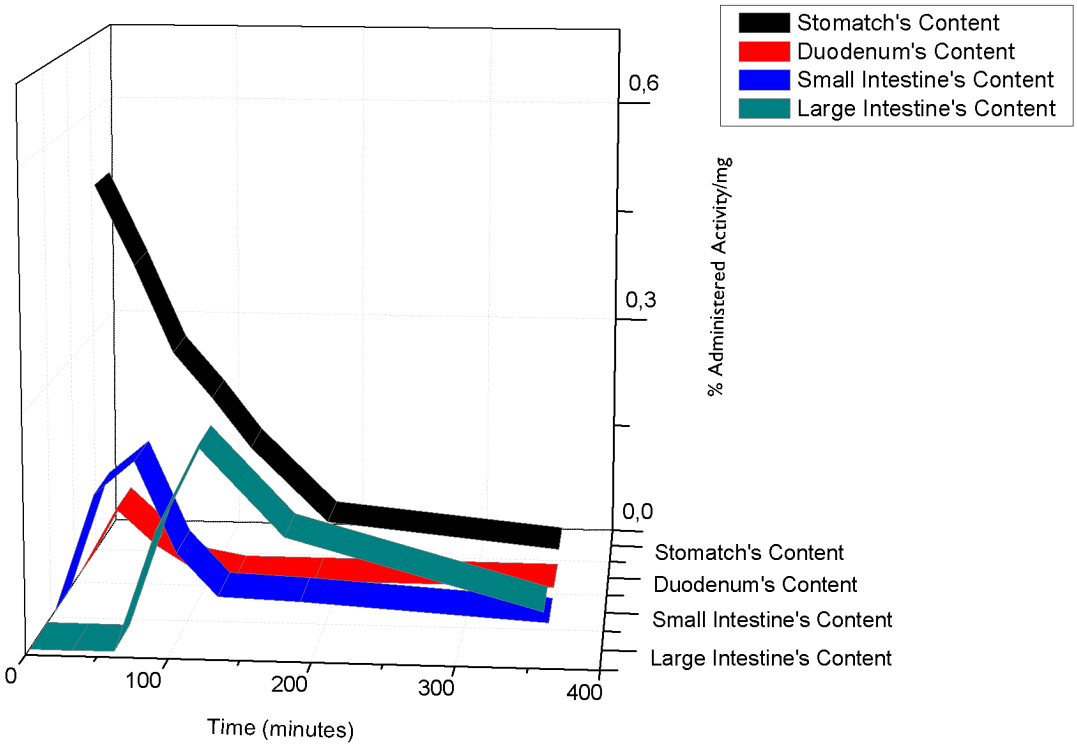


Figure 21 - The percentage administered activity/mg of $^{99m}$Tc-BSA in the gastrointestinal contents.

As illustrated above, the activity present in the stomach's content decreases over the time, reaching very low values 360 minutes after the administration. The duodenum's content achieves the activity peak 30 minutes after the administration followed by a quick elimination and reaching the lower values at 120 minutes. The peak of activity in the small intestine's content is attained 60 minutes after the administration and the lower values are obtained 360 after the administration. In the large intestine's content the maximum value occurs 120 minutes after the administration and 360 minutes after a considerable activity is still present.

Other organs and fluids beyond gastrointestinal tract were collected to study the intestinal absorption of $^{99m}$Tc-BSA. The results obtained are shown in the figure 22 where we can see that the radiopharmaceutical is only uptaken by the liver. $^{99m}$Tc-BSA uptake by the liver is very low and only occurs 120 minutes after administration and is maintained, at least, for more 60 minutes. After 360 minutes radiopharmaceutical uptake is no longer observed in the liver.

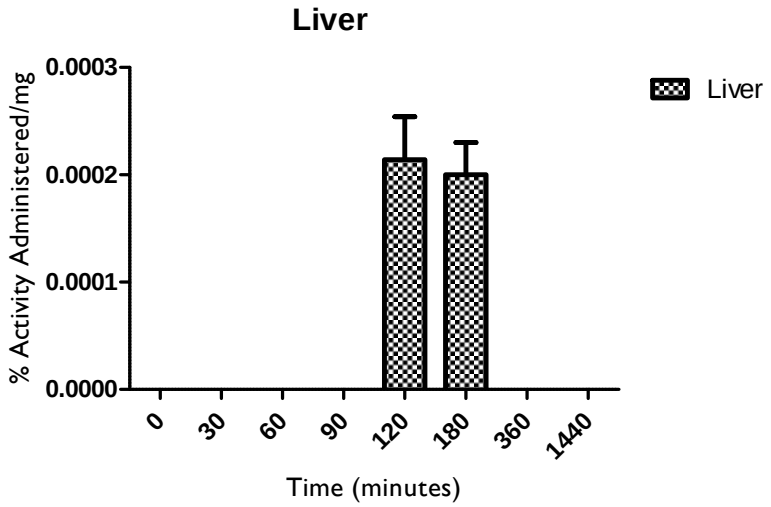


Figure 22 - The percentage administered activity/mg of $^{99m}$Tc-BSA in the liver.

The ROIs drawn in the images of the cages reveal a percentage of administered activity *per* mg equals to 0.0485(±0.0010) that corresponds to the eliminated contents (data not shown).

### 4.4.3 Quantitative analyses of $^{99m}$Tc-BSA-NP

After coating the NP with $^{99m}$Tc-BSA, the results of $^{99m}$Tc-BSA-NP biodistribution show its progression in the gastrointestinal tract for 1440 minutes. The percentage of administered activity *per* mg in the different organs and fluids studied is shown in figure 23.

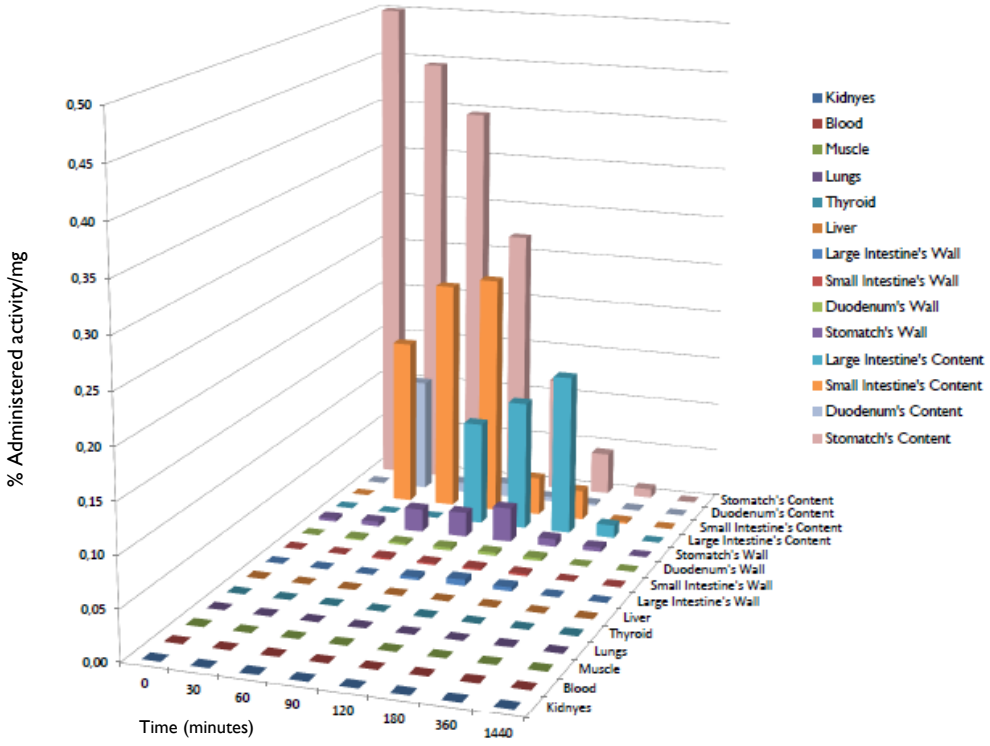


Figure 23 - Biodistribution in percentage of administered activity/mg of $^{99m}$Tc-BSA-NP.

The values correspondent to the figure 23 are in annex 2. The percentage of administered activity *per* mg in the stomach's content is the maximum value, since it is the local of administration. The activity present in the organs and fluids beyond gastrointestinal tract is minimal. The activity present in the gastrointestinal wall has the higher values in the stomach's wall. Related to the activity present in the stomach's content, it decreases over time, however, the complete elimination is only seen 1440 minutes after the administration. The activity in the intestine's content increases over the time and the $^{99m}$Tc-BSA-NP progression and its elimination can be appreciated. The complete radiopharmaceutical elimination is only reached 1440 minutes after the administration.

Figure 24 displays the percentage of administered activity per mg for each gastrointestinal wall for 360 minutes.

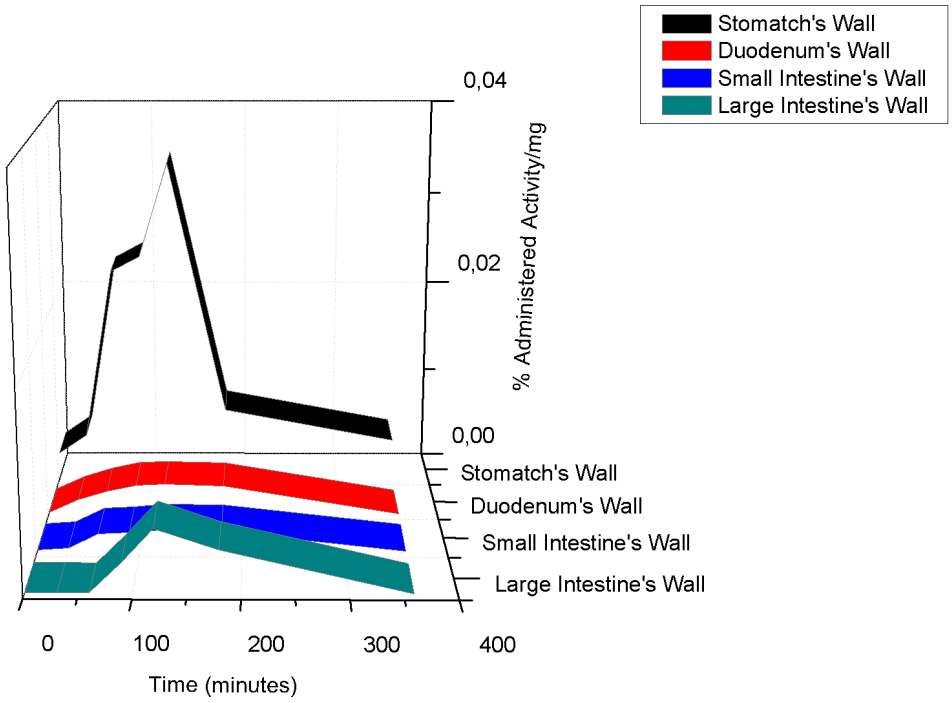


Figure 24 - The percentage administered activity/mg of $^{99m}$Tc-BSA-NP in the gastrointestinal wall.

Activity present in the stomach's wall achieves the maximum value at 120 minutes after the administration with a marked decrease within 30 minutes. The higher activity in the duodenum's wall is attained at 120 minutes after the administration. The same timings were obtained for the small intestine's wall. At 360 minutes after the administration the radiopharmaceutical elimination is complete from the duodenum's wall and the activity present in the small intestine's wall achieves the minimal values. The large intestine's wall has a peak of activity 120 minutes after the administration and at 360 minutes the complete radiopharmaceutical elimination was observed.

The figure 25 shows the percentage of administered activity *per* mg in the content of each portion of gastrointestinal tract for 360 minutes.

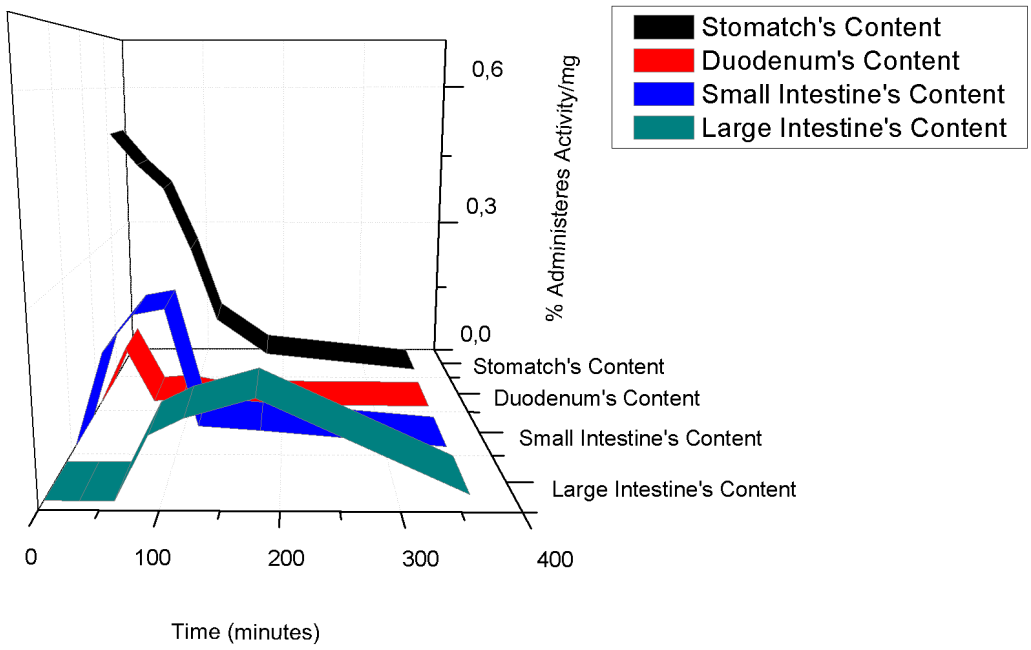


Figure 25 - The percentage of administered activity/mg of $^{99m}$Tc-BSA-NP in the gastrointestinal contents.

Activity present in the stomach's content decreases over the time reaching a lower value around 360 minutes after the administration. The duodenum's content achieves the activity peak 30 minutes after the administration with an elimination that reaches minimal values at 120 minutes. The peak of activity in the small intestine's content is attained 90 minutes after the administration whilst a lower value was obtained at 360 minutes. In the large intestine's content, the maximum value occurs 180 minutes after the administration and at 360 minutes a considerable activity is present in its content.

The organs and fluids beyond gastrointestinal tract were collected to study the intestinal absorption of $^{99m}$Tc-BSA-NP. Related to this radiopharmaceutical, the liver and the kidneys show very small uptake, and the results are shown in the figure 26.

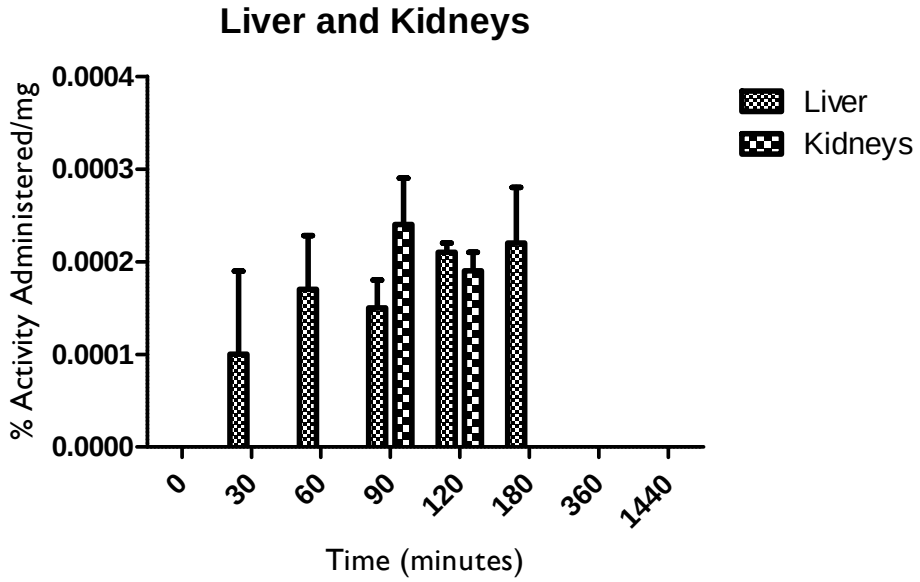


Figure 26 - The percentage of administered activity/mg of $^{99m}$Tc-BSA-NP in the liver and in the kidneys.

As shown in the figure 26 the uptake by the liver occurs 30 minutes after the administration and the uptake value is maintained for more 150 minutes, at least. At 360 minutes after the administration no uptake is observed in liver. Ninety minutes after the administration is possible see activity in the kidneys that decreases after 30 minutes.

The ROIs drawn in the cage images reveal a percentage of administered activity *per* mg equals to 0.0210(±0.0033) that corresponds to the eliminated contents (data not shown).

### 3.4.4 Comparative study

The purpose of the $^{99m}$Tc-BSA biodistribution study is to compare it with the obtained for $^{99m}$Tc-BSA-NP. Thus, next figures aimed to analyze differences between the profile of both radiopharmaceuticals.

The figure 27 illustrates differences in the activity present in the stomach's wall that are statistically significant until 180 minutes after administration. In fact, the p values obtained in the first 30 minutes and at 120 and 180 minutes after the administration were <0.001, and at 90 min was <0.05. Values obtained 60 and 360 minutes after the administration reveal no differences.

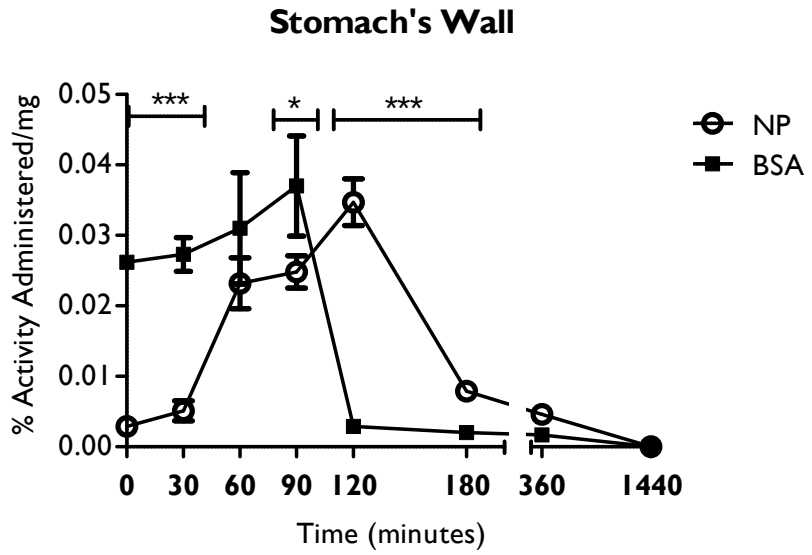


Figure 27 - The percentage of administered activity/mg calculated in the stomach's epithelium for $^{99m}$Tc-BSA and $^{99m}$Tc-BSA-NP. For each time the percentage activity administered/mg of $^{99m}$Tc-BSA was compared with the percentage activity administered/mg of $^{99m}$Tc-BSANP. Significant differences are indicated by * corresponding to $p<0.05$ and *** $p<0.001$.

In the duodenum's wall, as shown in the figure 28, the radiopharmaceuticals behavior is similar showing differences statistically significant only for the values obtained at 120 and 180 minutes after the administration ($p<0.01$ and $p<0.001$, respectively).

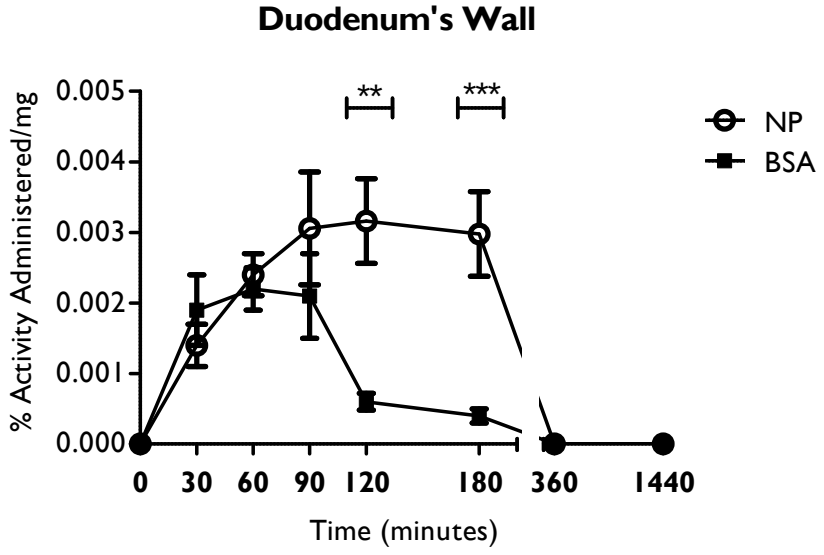


Figure 28 - The percentage of administered activity/mg calculated in the duodenum's epithelium for $^{99m}$Tc-BSA and $^{99m}$Tc-BSA-NP. For each time the percentage activity administered/mg of $^{99m}$Tc-BSA was compared with the percentage activity administered/mg of $^{99m}$Tc-BSANP. Significant differences are indicated by ** corresponding to $p<0.01$ and *** $p<0.001$.

The figure 29 is related to the small intestine's wall and the results show different statistical significance at the 30 and 60 minutes ($p<0.05$), 120 minutes ($p<0.01$) and 180 minutes ($p<0.05$) after the administration.

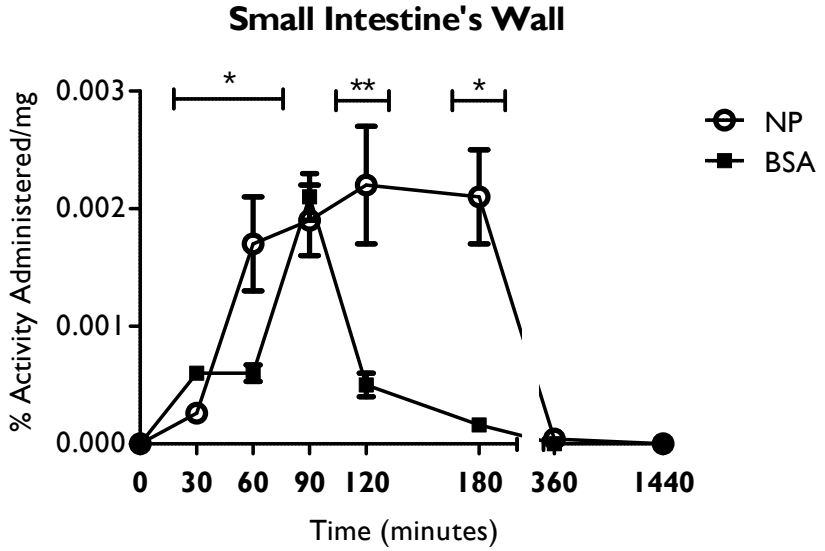


Figure 29 - The percentage of administered activity/mg calculated in the small intestine's epithelium for $^{99m}$Tc-BSA and $^{99m}$Tc-BSA-NP. For each time the percentage activity administered/mg of $^{99m}$Tc-BSA was compared with the percentage activity administered/mg of $^{99m}$Tc-BSANP. Significant differences are indicated by * corresponding to $p<0.05$ and ** $p<0.01$

In the large intestine's wall, that reflects the radiopharmaceuticals progression profile, and shown in the figure 30, there are statically significant differences only at 180 minutes after the administration ($p<0.001$).

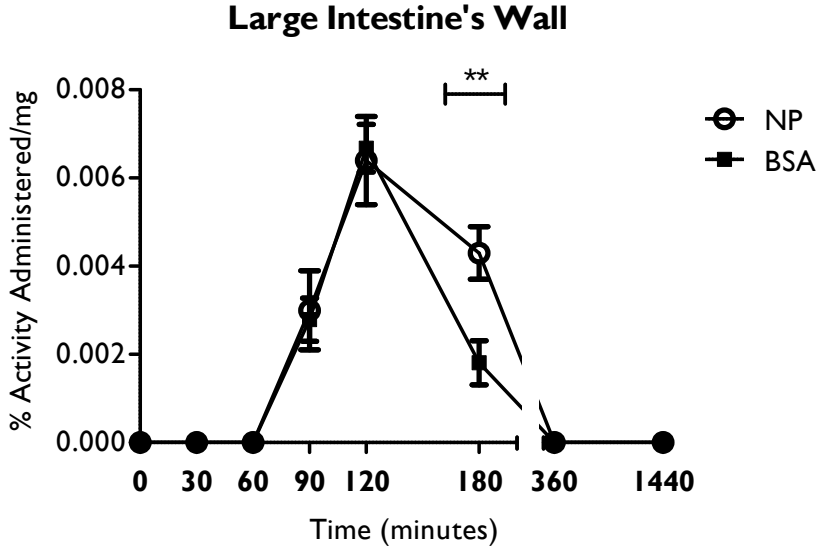


Figure 30 - The percentage of administered activity/mg calculated in the large intestine's epithelium for $^{99m}$Tc-BSA and $^{99m}$Tc-BSA-NP. For each time the percentage activity administered/mg of $^{99m}$Tc-BSA was compared with the percentage activity administered/mg of $^{99m}$Tc-BSANP. Significant differences are indicated by ** corresponding to $p<0.01$.

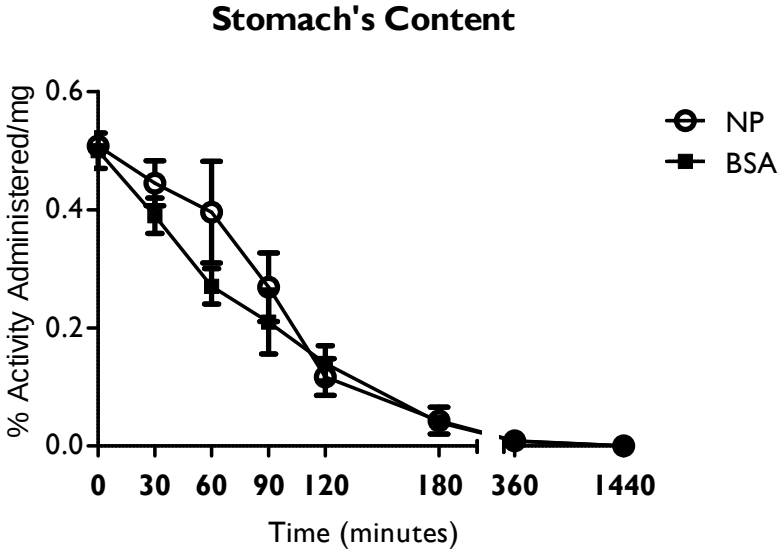


Figure 31 - The percentage of administered activity/mg calculated in the stomach's content for $^{99m}$Tc-BSA and $^{99m}$Tc-BSA-NP. For each time the percentage activity administered/mg of $^{99m}$Tc-BSA was compared with the percentage activity administered/mg of $^{99m}$Tc-BSANP.

The figure 31 illustrates the absence of statistically significant differences between the radiopharmaceuticals on stomach's contents. Similarly, in the duodenum's contents, there are only statistically significant differences at 60 minutes after the administration ($p<0.001$), as can be seen in the figure 32.

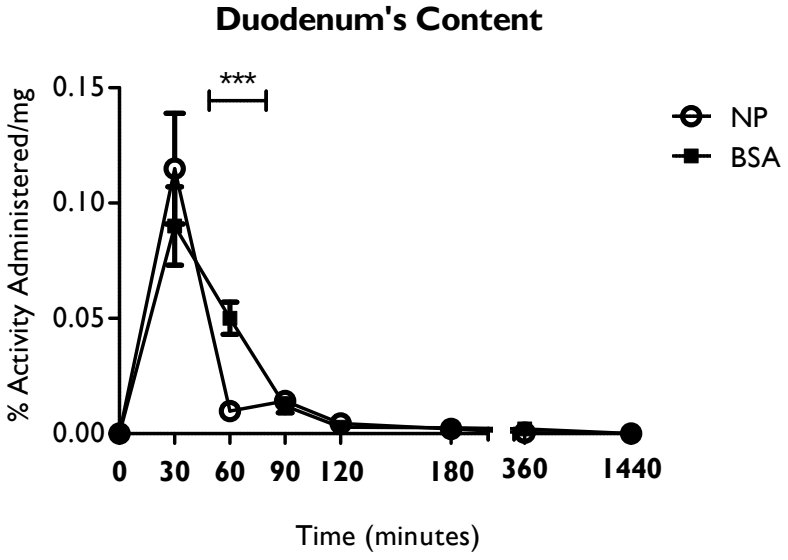


Figure 32 - The percentage of administered activity/mg calculated in the duodenum's content for $^{99m}$Tc-BSA and $^{99m}$Tc-BSA-NP. For each time the percentage activity administered/mg of $^{99m}$Tc-BSA was compared with the percentage activity administered/mg of $^{99m}$Tc-BSA-NP. Significant differences are indicated by *** corresponding to $p<0.001$.

Figure 33 compare the results of the small intestine´s contents, and we can see that the radiopharmaceuticals elimination is similar, but showing statistically significant difference ($p<0.001$) for the 90 minutes after the administration.

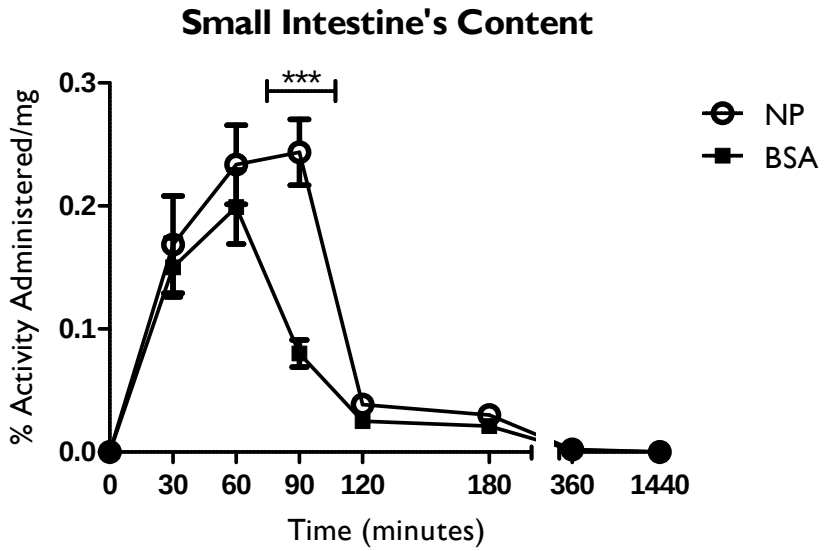


Figure 33 - The percentage of administered activity/mg calculated in the small intestine's content for $^{99m}$Tc-BSA and $^{99m}$Tc-BSA-NP. For each time the percentage activity administered/mg of $^{99m}$Tc-BSA was compared with the percentage activity administered/mg of $^{99m}$Tc-BSA-NP. Significant differences are indicated by *** corresponding to $p<0.001$.

The large intestine's contents elimination has statistically significant differences ($p<0.01$) only at 120 minutes after the administration, as illustrated in the figure 34.

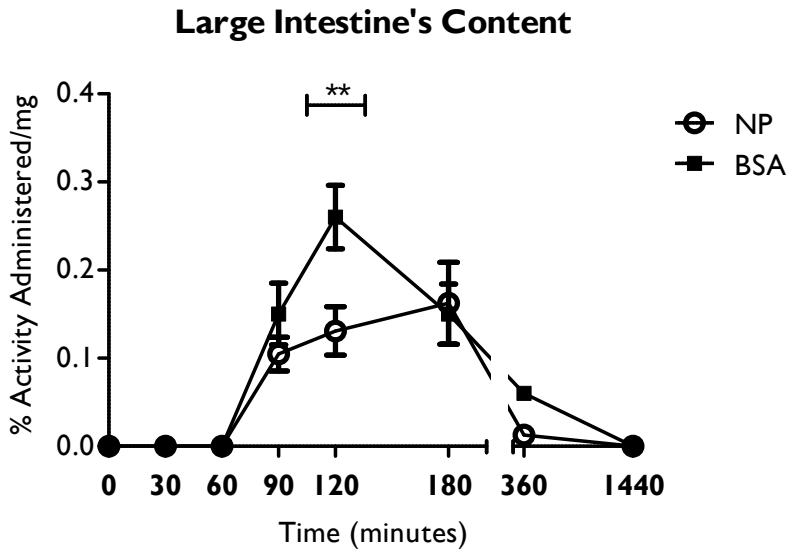


Figure 34 - The percentage of administered activity/mg calculated in the large intestine's content for $^{99m}$Tc-BSA and $^{99m}$Tc-BSA-NP. For each time the percentage activity administered/mg of $^{99m}$Tc-BSA was compared with the percentage activity administered/mg of $^{99m}$Tc-BSA-NP. Significant differences are indicated by ** corresponding to $p<0.01$.

# 5. Discussion and Conclusions

NP have been considered for oral administration of several molecules, such as proteins, enzymes, drugs, by facilitating delivery and absorption in the target site and by stabilizing and ensuring biological activity when required during gastrointestinal transit (WILCZEWSKA, 2012). The NP studied in this work are formulated by emulsification/internal gelation method in which nanoparticle contains a nucleus of calcium cross-linked alginate, dextran sulfate and insulin, following complexation with chitosan, being the outermost composed BSA. The BSA increases the stability of alginate-NP and consists of a protease-protective protein (HURTEAUX, 2005; SCHECHTER, 2005; WOITISKI, *et. al.*, 2009a; WOITISKI, *et. al.*, 2009b).

The aim of this work was to study the biodistribution of insulin-loaded BSA-coated NP. As their external coat is BSA, BSA was radiolabeled with $^{99m}$Tc before coating NP. Therefore, BSA was radiolabed and a quality control procedure was developed and optimized. Another purpose of this study is the monitoring of NP while passing through gastrointestinal tract, namely contribute to better understand its degradation and mucoadhesive properties. Based on a comparison between the biodistribution studies obtained with the $^{99m}$Tc-BSA and $^{99m}$Tc-BSA-NP, some considerations are presented in this chapter.

The development and optimization of BSA radiolabeling was the first step in which the optimization of the quality control procedure was the first approach in order to determine the radiochemical purity of $^{99m}$Tc-BSA. Despite radiolabeling of HSA, namely with $^{99m}$Tc has been studied, its quality control is poorly documented, in respect of $^{99m}$Tc-RH quantification (ZOLLE, *et. al.*, 1973; RHODES, 1974; KLEISNER, *et. al.*, 2000; WANG, *et. al.*, 2011). According to $^{99m}$Tc-HSA quality control procedures available in literature and specifically concerning $^{99m}$Tc-RH quantification there are two options of $R_f$ value in the chromatographic systems in order to isolate $^{99m}$Tc-RH. In the first option, it is possible to consider the $R_f$ value of $^{99m}$Tc-BSA different of zero and a $^{99m}$Tc-RH $R_f$ value equal to zero; in the second option it is possible to consider $^{99m}$Tc-BSA $R_f$ value equal to zero and a $^{99m}$Tc-RH $R_f$ value different of zero. Based on this, and considering literature review, the mobile phase consisting of ACD was tested in different chromatographic strips in order to establish a quality control system in which the $^{99m}$Tc-RH $R_f$ value was different of zero (OZGUR, *et. al.*, 2011). As the stationary phase suggested by the literature was not available in Biophysics Department, other stationary phases were tested, namely Aluminum SG 60, Aluminum Oxide IB-F, ITLC-SG and Whatmman 31 ET. The chromatographic system with ACD as mobile phase and ITLC-SG as stationary phase resulted in a $^{99m}$Tc-RH $R_f$ value between 0.5

and 1, allowing the $^{99m}$Tc-RH isolation. Thus it was possible to optimize the quality control of BSA radiolabeling with $^{99m}$Tc in order to separate the possible impurities.

In the end of the 60´s and beginning of the 70´s there were already several studies available with $^{99m}$Tc-HSA. The radiolabeling procedure was largely studied, consequently there are several methods described (PERSSON and LIDÉN 1969; RHODES, 1974). Among these methods, the one that uses stannous chloride was the first choice, because it is widely used to prepare radiopharmaceuticals labeled with $^{99m}$Tc, and it is an easy, available and reproducible. The protocol that uses stannous chloride varies with the authors and the need of low pH during radiolabeling is not a prerequisite in all of them (WANG, *et. al.*, 2011). For this reason, and due to the requirement of the NP coating be performed with a BSA solution at pH 5.1, firstly the radiolabeling procedure was performed with no pH manipulation and stannous chloride was dissolved in ultrapure water (the solution pH was 5.0). An higher radiochemical purity was achieved 30 minutes after the radiolabeling. However, the reaction is not stable over time and the percentage of $^{99m}$Tc-RH rise up after 30 minutes.

The $^{99m}$Tc-RH formation occurs when a reduced $^{99m}$Tc molecule undergoes hydrolysis in aqueous solution. In this case, reduced $^{99m}$Tc reacts with water to form various hydrolyzed species depending on the pH, time duration of hydrolysis and presence of agents, like molybdenum and alumina. This hydrolysis competes with the chelation process of the desired compound and reduces the yield of $^{99m}$Tc-pharmaceutical (SAHA, 2004a). These reactions turns more probable when stannous chloride is used in aqueous solution at pH of 6.0 to 7.0. To prevent the hydrolysis of $Sn^{2+}$, before the reduction of technetium, can be used an adequate quantity of reducing agent and besides that it is important to avoid the presence of oxygen, air, or any oxidizing agent in the vial (SAHA, 2004a). As the procedures were carried out in purgated vials and the stannous chloride was dissolved in purgated water the presence of oxygen was minimized. Furthermore, the antioxidant used to avoid radiolysis is widely described in the radiopharmaceutical preparation, such as for methylene diphophonate (MDP) and hydroxymethylenediphosphonic acid (HDP) kits whose cold kit formulation contains ascorbic acid (SAHA, 2004a).

Taking in account the results obtained and the fact that ascorbic acid is used to stabilize the radiolabeling procedure and decrease the formation of $^{99m}$Tc-RH, the effect of this organic acid was studied by using the stannous chloride method. However the results obtained were not satisfactory due to low radiochemical purity. Even in the case of the higher radiochemical purity there was always a disadvantage regarding the incubation time or the stability of the reaction. Also the effect of the heating in the protocol with ascorbic acid did not produce positive results.

Furthermore, the pH influence in the radiolabeling efficiency was also tested based on other methods described to label albumin with Tc-99m (PERSSON and LIDÉN, 1969; RHODES, 1974). The iron-ascorbic acid method requires low pH values, ranging between 1 and 2 (PAOLI, *et. al.*, 1966; PERSSON and LIDÉN, 1969; RHODES, 1974) whereby the pH values of 1 or 2 were tested in the previous protocol composed by stannous chloride and ascorbic acid. The radiolabeling efficiency with a pH = 1 seems be too low, because, although the reaction being stable its radiochemical purity is lower compared to the radiochemical purity obtained with pH = 2. Even though the positive influence of pH decrease in the radiochemical purity, which almost achieved 90 %, these results were difficult to reproduce, as referred in the bibliography (PERSSON and LIDÉN, 1969).

Besides the methods with stannous chloride, a method that is described to prepare macroaggregates of HSA was also evaluated. The method consists in HSA radiolabeling with $^{99m}$Tc followed by heating at high temperature (90°C), which promotes particles aggregation. Thus, this method was reproduced to radiolabel BSA without the last step in order to obtain a suspension of $^{99m}$Tc-BSA particles (PAOLI, *et. al.*, 1966; CRAGIN, 1969). The results of the radiochemical purity were the pretended since the percentage of radiolabeling was higher than 96 % and remain stable for 360 minutes, which fulfills the requirements to proceed to the *in vivo* studies. Taking into account that this protocol requires heating steps and pH changes, the best solution to prevent NP from this stress was coating them with $^{99m}$Tc-BSA instead of radiolabeling the final NP. A further advantage of this procedure was mitigating the radiolabeling of other NP compounds allowing the comparative study between $^{99m}$Tc-BSA-NP and $^{99m}$Tc-BSA biodistribution. However, even with the addition of a buffer solution with a pH of 7.4, the final pH of the solution was still too low (pH = 2). Thereby, the pH increase of $^{99m}$Tc-BSA suspension was mandatory to allow efficient NP coating, since the isoelectric point of BSA is 4.7 (URBANO, 2004). The albumin coating of these NP is based in an electrostatic interaction with chitosan, which has a positive electric charge. Consequently, the BSA pH above isoelectric point is a requisite, since its functional groups must be negatively charged to interact with chitosan. Moreover, the NP coating at low pH could change the NP conformation since their polymeric matrix has pH-sensitive behavior. The pH variations affect the electric charge of insulin, which could be enough to decrease insulin entrapment (SARMENTO, *et. al.*, 2007b; WOITISKI, *et. al.*, 2009b). Since the influence of increasing pH to 5 after the radiolabeling of BSA was tested and no influence in the radiochemical purity was detected, the NP coating with $^{99m}$Tc-BSA at this pH was possible.

The NP formulation was optimized with a concentration of albumin adjusted according to several NP parameters, such as size, zeta potential and insulin entrapment. However,

during the production of NP, the percentage of albumin added to the NP suspension that actually interacts with the NP and the percentage that stays unbounded was unknown. Therefore, the available method to answer and solve this question was the centrifugation to separate the unbounded BSA combined with its quantification by Coomassie® Protein Assay Reagent Kit. This protocol revealed that a considerable percentage of BSA were not coating the NP since it was in the supernatant, after the coating step. The centrifugation protocol selected was the one with the lower time and rotation force applied capable of separate the maximum of unbounded BSA from the coated NP, in order to avoid aggregation, as much as possible. Therefore, the centrifugation was performed after the NP coating with $^{99m}$Tc-BSA in order to eliminate the $^{99m}$Tc-BSA that did not incorporate the nanoparticle, increasing the study specificity. Nevertheless, the NP sonication was carried out aiming the redispersion of NP in the suspension.

According to the aim of this work, to study the biodistribution of insulin-NP and regarding the *in vivo* studies of NP was important to ensure the similarity between NP and radiolabeled NP, considering specific characteristics, like size distribution. Into this matter, working with radioactivity has some limitations, since it requires special conditions. To overcome this point the NP were coated with $^{99}$Tc-BSA, which maintain the chemical properties of $^{99m}$Tc-BSA-NP. Thereby, size of either $^{99}$Tc-BSA-NP and BSA-NP was measured at the same conditions allowing the comparison. These results proved that radiolabeled BSA did not affect the NP characteristics, in respect of their size. However, other characteristics, such as zeta potential and insulin entrapment efficiency should be determined to verify the influence of the protocol used to radiolabel NP did not affect its characteristics relatively to the original NP (SARMENTO, *et. al.*, 2007a; SARMENTO, *et. al.*, 2007b; WOITISKI, *et. al.*, 2009b).

The *in vivo* studies were designed to ascertain the NP biodistribution, particularly in terms of gastrointestinal transit, since NP are intended for oral delivery. Taking in account that the nanoparticle radiolabeled constituent was BSA, the information obtained was specifically related with its biodistribution. However, the comparison of $^{99m}$Tc-BSA and $^{99m}$Tc-BSA-NP biodistribution allows inferring about NP biodistribution based on the differences between the two radiopharmaceuticals.

According to the NP purpose, the radiopharmaceuticals were administered by gavage. Besides the study with radiolabeled NP, the $^{99m}$Tc-BSA biodistribution was also performed after gavage administration, in order to allow the comparison and to ensure the same conditions. Since the increase of pH is a requirement to coat NP, $^{99m}$Tc-BSA was treated at

the same pH when administered to mice, to be possible to establish a correlation between both radiopharmaceuticals, which were in the same pH conditions.

The information provided by the gastrointestinal contents allows to infer about times of gastrointestinal transit. The percentage of administered activity *per* mg for each gastrointestinal portion had tight differences, which reveals a time of gastrointestinal transit similar for both radiopharmaceuticals. The gastric empting for both radiopharmaceuticals is gradual over time, which is concordant with the normal pattern of gastric retention after gavage administration (LUCENA, 2009).

The elimination of $^{99m}$Tc-BSA-NP from the small intestine to the large intestine seems to be slower than $^{99m}$Tc-BSA elimination, since the increase of activity in the large intestine is more gradual. Moreover, 90 minutes after the radiopharmaceuticals administration the activity present in the small intestine for $^{99m}$Tc-BSA was around half of the activity present in the small intestine for $^{99m}$Tc-BSA-NP (figure 33). In general, in humans, a molecule takes around 200 minutes to complete its intestinal progression after arrives to the cecum (KIM, 1968; HUNG, 2006). The small intestine transit time for both radiopharmaceuticals, which reflects the intestinal progression, was between 90 and 120 minutes. Although the differences presented in their progression profiles, both achieved similar values of percentage of administered activity *per* mg in the small intestine's contents at the same time. Taking into account that the metabolism of mice is faster than humans, these results seem to correspond to a normal transit time.

The presence of the $^{99m}$Tc-BSA-NP in the gastrointestinal wall reveals the NP adhesion properties. Contrary to what was observed in the gastrointestinal contents, the activity in the intestinal walls presented significant differences in the stomach, duodenum and small intestine, when the two radiopharmaceuticals, $^{99m}$Tc-BSA and $^{99m}$Tc-BSA-NP, are compared.

The $^{99m}$Tc-BSA present in the stomach wall in mice studied immediately after the administration was 70 % of its maximum value. This fact reveals a quickly retention of this radiopharmaceutical in the stomach epithelium. One hundred and twenty minutes after $^{99m}$Tc-BSA administration the activity present in the stomach wall roughly decreased comparing with the stomach wall activity observed 30 minutes before (90minutes after $^{99m}$Tc-BSA administration; figure 27). These results suggest that the radiopharmaceutical retention in the stomach wall was not proportional to the radiopharmaceutical present in the content, since the decrease of the percentage of administered activity *per* mg in this content was not so accentuated. The percentage of administered activity *per* mg in the stomach wall after $^{99m}$Tc-BSA-NP administration only achieved the same higher values obtained by $^{99m}$Tc-BSA immediately after the administration, 60 minutes after $^{99m}$Tc-BSA-NP

administration (figure 27). Taking in account that the percentage of administered activities *per* mg in the first 30 minutes represent only 8 % of the maximum values obtained for $^{99m}$Tc-BSA-NP in the stomach wall and simultaneously the percentage of administered activities *per* mg of both radiopharmaceutical after 60 minutes are similar, it demonstrates that there is a possible late release of $^{99m}$Tc-BSA from the $^{99m}$Tc-BSA-NP, that has available to reach the stomach epithelium. According to stomach pH the albumin was positive electric charge. Therefore, the $^{99m}$Tc-BSA release from the NP is based in charges repulsion, since the chitosan is positively charged (WOITISKI, *et. al.*, 2009a).

The percentage of administered activity *per* mg of $^{99m}$Tc-BSA in the duodenum's wall obtained 30 minutes after the administration was fairly near to the maximum peak value, remaining constant up to 90 minutes after the administration. The decrease of percentage of administered activity *per* mg of $^{99m}$Tc-BSA in the duodenum's wall revealed the same excretion profile of duodenum's content. This fact suggests similarities on the behavior of $^{99m}$Tc-BSA in the duodenum content and wall. The values of percentage of administered activity *per* mg obtained in the study of $^{99m}$Tc-BSA-NP in the duodenum's epithelium was similar to the values obtained with $^{99m}$Tc-BSA, since no significant differences were observed in the first 90 minutes of the study. However, the presence of $^{99m}$Tc-BSA-NP in the duodenum's wall was maintained in the same value until 180 minutes after the administration, contrary to the verified with $^{99m}$Tc-BSA in which there was a decrease after 90 minutes (figure 28). In other words, the presence of $^{99m}$Tc-BSA-NP in the duodenum's wall was maintained even after the radiopharmaceutical elimination from duodenum´s content, at 90 minutes. These results suggest that BSA maintain its interaction with NP or with NP constituents until 180 minutes after radiopharmaceutical administration. The adhesion of NP to the intestinal epithelium is expected according to the mucoadhesive properties of its constituents, namely, chitosan and alginate. The duodenum presents a basic pH, which triggers insulin release from NP according to the isoelectric point of insulin and its electrostatic interaction with alginate (SARMENTO, *et. al.*, 2007a; SARMENTO, *et. al.*, 2007b; WOITISKI, *et. al.*, 2009a; WOITISKI, *et. al.*, 2009b). The BSA coating was designed to be a sacrificial-target in the stomach providing nanoparticle protection and avoiding the chitosan exposition to the stomach pH and consequently decreasing insulin release (WOITISKI, *et. al.*, 2009a; WOITISKI, *et. al.*, 2009b). BSA interaction with mucoadhesive polymers in the duodenum can explain the difference between the results obtained for the radiopharmaceuticals. At duodenum pH, the BSA interaction is probably with chitosan, since these compounds present opposite electrical charge, while the electrical charges of BSA and alginate are both negative. Actually, the values of percentage of administered activity *per* mg

in duodenum's wall were very low, representing around 3 % of the maximum value obtained in the duodenum's content (figure 28). Thus, even that the apparent BSA interaction with chitosan had influence on insulin retention, it would not compromise insulin release in duodenum, considering the low values of the $^{99m}$Tc-BSA-NP present in the duodenum´s wall.

The percentage of administered activity *per* mg of $^{99m}$Tc-BSA in the small intestine's wall has a peak 90 minutes after the radiopharmaceutical administration. The activity peak in the small intestine's contents occured 60 minutes after the radiopharmaceutical administration, and in the next 30 minutes approximately half of the radiopharmaceutical moves to the large intestine (figures 29 and 33). These results suggest that the activity present in the wall was not proportional to the activity existent in the contents of the small intestine. Therefore, the results obtained with the small intestine's wall could be explained by the radiopharmaceutical location along the small intestine. By other words, 90 minutes after the radiopharmaceutical administration the majority of the radiopharmaceutical present in the small intestine was in its distal portion. During the experimental work it was clear an alteration of the consistency of the intestinal content, what was related with the water absorption that occurs along the intestinal tract. Moreover, the high number of intestinal villus increases the intestinal epithelium surface, which can potentiate the radiopharmaceutical retention. The presence of intestinal villus allied to the more solid content consistency can justify the peak of activity present in the small intestine's wall because both factors difficult the epithelium washing during biodistribution studies.

The retention of $^{99m}$Tc-BSA-NP in the small intestine's wall reaches a percentage of administered activity *per* mg at 60 minutes that was maintained until 180 minutes after the administration. This radiopharmaceutical reached to the small intestine 30 minutes after the administration with a percentage of administered activity *per* mg in the small intestine's content that surrounded 70% of the maximum value obtained to this content, although the peak only was 90 minutes after administration (figure 28). These results suggested that the radiopharmaceutical retention in the small intestine's wall did not occur immediately after the radiopharmaceutical contact with the wall. Furthermore, the interaction between this radiopharmaceutical and this wall was maintained for the following 60 minutes, at least, after the radiopharmaceutical present in the content elimination to the large intestine. For the reasons mentioned above to the duodenum's wall, these results suggested some interaction between BSA and chitosan that potentiate the radiopharmaceutical retention in the small intestine's wall, even after the content progression. The values obtained in this wall are similar to the values obtained in the duodenum's wall suggesting that the interaction

between BSA and chitosan are stable along the intestinal progression, although it only represents a little percentage of the administered radiopharmaceutical.

The results obtained concerning large intestine's wall and content were very similar for both radiopharmaceuticals, presenting the same profile (figure 29). Thus, the results suggested correlation between the presences of the radiopharmaceutical in the wall with the activity present in the content. The fact of the values of percentage of administered activity *per* mg obtained in the large intestine's wall surrounded the triple of the values obtained in the other intestinal walls can be explained by the cecum anatomy and the consistency of the content, both for difficult the washing of the large intestine wall.

The total elimination of both radiopharmaceuticals was supported by the absence of any counts in the static images acquired in the mice 1440 minutes after administration (figures 15 and 16), and also because of the presence of activity in the feces existent in the cages, at the same time. The low values of the percentage of administered activity *per* mg obtained are explained by radionuclide decay, since 1440 minutes after the administration already passed four $^{99m}$Tc half-times. Besides that and corroborating the results obtained for quality control it is possible to observe that there is no thyroid uptake (figures 19 and 23).

Looking to the results obtained in the organs and fluids studied to evaluate the intestinal absorption at radiopharmaceuticals, the first consideration is focused in the fact that the values of the percentage administered *per* mg that are very low, surrounding 0.04% of the values obtained in the stomach's content immediately after the administration. Thus, liver and kidney uptake was not significant.

The obtained results reveal that the radiolabeling of BSA and BSA-NP with $^{99m}$Tc and its quality control was optimized, since the radiolabeling efficiency obtained was higher than 96 %, stable for 360 minutes and it was reproducible.

Considering that albumin it is a sacrificial-target designed to protect the insulin-loaded NP in the stomach, the *in vivo* studies did not allow to conclude about the insulin absorption. A possible strategy to access this information is to label insulin with a radionuclide and through the nuclear medicine tools track its biodistribution after oral NP administration. According to the literature, the insulin has already been radiolabeled with single photons emitters, such as $^{67}$Ga, $^{123}$I and $^{99m}$Tc, and with positron emitters, like $^{18}$F (DOZIO, 1992; AWASTHI, *et. al.*, 1994; GUENTHER, *et. al.*, 2006; JALILAN, 2007).

Furthermore, considering the results observed and discussed, the differences between both radiopharmaceuticals suggested that not all of albumin was degraded in the stomach. Therefore, these results still give valid and fruitful information about NP transit in the gastrointestinal tract. Previous insulin release studies (data not shown) revealed that NP

achieved insulin total release 180 minutes after contact with simulated intestinal fluid. Moreover, considering that the *in vivo* studies reveal a time of small intestinal transit ranging between 90 and 120 minutes, a possible approach, to the nanoparticle optimization, was increase the permanency of NP in the small intestine.

# 6. Bibliography

AKDOGAN, Y., REICHENWALLNER, J., HINDERBERGER, D. (2012). "Evidence for water-tuned structural differences in proteins: an approach emphasizing variations in local hydrophilicity." Lister Hill National Center for Biomedical Communications.

AL-TABAKHA, M. M., ARIDA, A. I. (2008). "Recent Challenges in Insulin Delivery Systems: A Review." Indian J Pharm Sci. **70**(3):278-286.

Alternative Devices for taking insulin in Diabetes guide today. Accessed on 23rd June 2014. Available on internet: http://diabetesguidetoday.com/alternative-devices-for-taking-insulin/

ARSHADY, R. (1990). "Albumin microspheres and microcapsules: methodology of manufacturing techniques." J. Control. Rel. **14**: 111-131.

AWASTHI, V. [*et.al.*] (1994). "99mTc—Insulin: Labeling, biodistribution and scintiimaging in animals." Nuclear Medicine and Biology **21**(2): 251-254.

BANERJEE, S., PILLAI, M. R., RAMAMOORTHY, N. (2001). "Evolution of Tc-99m in diagnostic radiopharmaceuticals." Sem Nucl Med **31**(4): 260-277.

BRANGE, J. (1987). Galenics of insulin: the physico-chemical and pharmaceutical aspects of insulin and insulin preparations, Springer-Verlag.

BURTING, P. (2003). "Nutritional value of seaweeds." EJEAFChe **2**: 498-503.

CERNEA, S., RAZ, I. (2006). "Noninjectable methods of insulin administration." Drugs of Today **42**(6):405.

COLEMAN, R. E. (2006). Reimbursement for PET and PET/CT imaging. PET/CT - Essentials for Clinical Practice. R. E. WORKMAN, COLEMAN, R. R. USA, Springer**:** 23-32.

CRAGIN, M. D., WEBBER, M. M., VICTERY, W. K., PINTAURO, D. (1969). "Technique for rapid preparation of lung scan particles using 99mTc-sulfur and human serum albumin." The journal of Nuclear Medicine **10**: 621-623.

CUI, F. [*et.al.*]. (2004). "A study of insulin-chitosan complex NP used for oral administration." j. Drug Del. Sci. Tech **14**:435-439.

DAMGÉ, C., VRANCKX, H. [*et.al.*] (1997). "Poly(alkyl cyanoacrylate) nanospheres for oral administration of insulin." Journal of Pharmaceutical Sciences **86**(12): 1403-1409.

DE PAOLI, T. [*et.al.*] (1966). "Albumin macroaggregates labelled with Tc99m." The International Journal of Applied Radiation and Isotopes **17**(9): 551-552.

DESCRITOFORO, C., ZOLLE, I. (2007). Quality control methods for 99mTc Radiopharmaceuticals. In: Zolle, I.. Technetium-99m Pharmaceutials: Preparations and Quality Control in Nuclear Medicine. Berlin, Springer. 123-149.

DOZIO, N. [*et.al.*] (1992). "In vivo demonstration of insulin-receptor defect with 123I-labeled insulin and scintigraphic scanning in severe insulin resistance." Diabetes Care **15**(5): 651-656.

ELSINGA, P. [*et.al.*] (2010). Guidance on current good radiopharmacy parctice (cGRPP) for the small-scale preparation of radiopharmaceuticals E. J. N. M. M. Imaging, Springer.

GEISS, M. M. E. A. L. S. (2000). The Burden of Diabetes Mellitus. In: N. G. C. JacK L. Leahy, William T. Cefalu.Medical Management of Diabetes Mellitus. New York, USA, Marcel Dekker, Inc. 1-17.

GITTOES, N. J. L. [*et.al.*] (2010). Drug-Induced Diabetes. Textbook of Diabetes, Wiley-Blackwell**:** 265-278.

GOMBOTZ, W. R., WEE, S. F. (1998). "Protein release from alginate matrices." Adc. Drug Deliv. **31**:267-285.

GORDON STILL, J. (2002). "Development of oral insulin: progress and current status." Diabetes/Metabolism Research and Reviews **18**(S1): S29-S37.

GUENTHER, K. J. [*et.al.*] (2006). "Synthesis and in Vitro Evaluation of 18F- and 19F-Labeled Insulin: A New Radiotracer for PET-based Molecular Imaging Studies." Journal of Medicinal Chemistry **49**(4): 1466-1474.

HANEMANN, T., SZABÓ, D. V. (2012). "Polymer-NP composites: from synthesis to modern application." materials **3**:3468-3517.

HOSNY, E. A., GHILZAI, N. M. K., AL-DHAWALIE, A. H. (1995). "Effective intestinal absorption of insulin in diabetic rats using enteric coated capsules containing sodium salicylate." Drug Dev. Ind. Pharm **21**:1583-1589.

How to give an insulin injection in Phartoonz, A cartoonized pharmacology! Accessed on 23rd June 2014. Available on internet: http://www.phartoonz.com/2010/10/24/how-to-give-an-insulin-injection/

HUNG, G., TSAI, C., LIN, W. (2006). "Development of a new method for small bowel transit study." Annals of Nuclear Medicine **20**(6): 387-392.

HURTEAUX, R. [*et.al.*] (2005). "Coating alginate microspheres with a serum albumin-alginate membrane: application to the encapsulation of a peptide." Eur. J. Pharm. **24**: 187-197.

INTERNATIONAL ATOMIC ENERGY AGENCY, I. A. E. A. (2006). Quality assurance for Radioactivity Measurement in Nuclear Medicine. Technical reports series no. 454. I. A. E. A. Vienna**:** 19-32.

JADVAR, H., PARKER, J. A. (2005). PET radiotracers. Clinical PET and PET/CT. H. JADVAR, PARKER, J. A. USA, Springer**:** 45-68.

JALILAN, A. [*et.al.*] (2007). "Preparation and biodistributio of [67Ga]-insulin for SPECT purposes." Nukleonika **52**(4): 145-151.

JAWAHAR, N., MEYYANATHAN, SN. (2013). "Polymeric NP for drug delivery and targeting: A comprehensive review." International Journal of Health & Allied Sciences **1**(4):217-223.

JUNG, T. [*et.al.*] (2000). "Biodegradable NP for oral delivery of peptides: is there a role for polymers to affect mucosal uptake?" Eur. J. Pharm. Biopharm. **50**:147-160.

KAYANI, I. [*et.al.*] (2008). "Functional imaging of neuroendocrine tumors with combined PET/CT using 68Ga-DOTATATE (DOTA-DPhe1,Tyr3-octreotate) and 18F-FDG." Cancer **112**(11): 2447-2455.

KIM, S. K. (1968). "Small intestine transit time in the normal small bowel study." **104**(3).

KLEISNER, I. [*et.al.*] (2000). The use of redox polymers in labelling procedures of proteins and peptides with 99mTc. I. Properties of redox polymers and technique of labelling.

KNOWLER, P. H. B. A. W. C. (2005). Definition, Diagnosis, and Classification of Diabetes Mellitus and Glucose Homeostasis. In: L. W. Wilkins. Joslin's DIABETES MELLITUS. Boston, MA**.** 331-338.

LENCKI, R. W. J., NEUFELD, R. J., SPINNEY, T. (1989). Method of producing microspheres. USA. **5:**822-834.

LENTLE, B., CELLER, A. (2003). An introduction to nuclear medicine. In: W. D. Leslie, Greenberg, I. D.Nuclear Medicine., Landes Bioscience**.** 1-14.

LIU, X. D. [et.al] (2002a). "Preparation of uniform calcium alginate gel beads by membrane emulsification coupled with internal gelation." J. Appl. Polym. Sci. **87**: 848-852.

LIU, X. D. [*et.al.*] (2002b). "Characterization of structure and diffusion behavior of Ca-alginate beads prepared with external or internal calcium sources." J. Microencapsul. **19**: 775-782.

LIU, Y., TSENG, Y., HUANG, L. (2012). "Biodistribution studies of NP using fluorescence imaging: a qualitative or quantitative method?" Pharm Res. **29**(12): 3273-3277.

LUCENA, F. (2009). Desenvolvimento de radiofármaco para estudo não invasivo do trânsito intestinal. Master, Universidade de Lisboa.

MAHAMOOD, A., JONES, A. (2003). Tehnetium Radiopharmaceuticals. Handbook of radiopharmaceuticals. Radiochemistry and application. M. Welch, Redvanly, C. West Sussex, John Wiley & Sons Ltd.**:** 323-362.

MAHER, K. [*et.al.*] (2004). Basic Physics of Nuclear Medicine. In: K. e. a. MAHER, Wikibooks**:** 63-93.

McCONVILLE, P. [*et.al.*] (2013). "New learning: Advancing drug discovery and development through non-invasive biodistribution imaging." Molecular Imaging.

Medtronic MiniMed Paradigm Insulin Pumps Lawsuit in Stainberg Law Firm P.C. Accessed on 23rd June 2014. Available on internet: http://www.thesteinberglawfirm.com/medtronic/contact.htm

ONAL, S., ZIHNIOGLU, F. (2002). "Encapsulation of insulin in chitosan-coated alginate gel beads: oral therapeutic delivery." Artif. Cells Blood Substit. Immobil. biotechnol. **30**:229-237.

OPPENHEIM, R. C., [*et.al.*] (1982). "Production and evaluation of orally administered insulin NP." Drug Dev. Ind. Pharm **8**:531-546.

Ozgur, A. [*et.al.*] (2011). Synthesis and biological evaluation of radiolabeled photosensitizer linked bovine serum albumin NP as a tumor imaging agent.

PEPPAS, N. A., KAVIMANDAN, N. J. (2006). "Nanoscale analysis of protein and peptide absorption: insulin using complexation and pH-sensitive hydrogels as delivery vehicles. ." Eur. J. Pharm. Sci. **29**:183-197.

PERSSON, R. B. R. and K. LIDÉN (1969). "99mTc-labelled human serum albumin: A study of the labelling procedure." Int J Appl Radiat Isot **20**(4): 241-248.

Pharmjet introduces needle-free subcutaneous and intramuscular injectors in Gadget dite. Accessed on 23rd June 2014. Available on internet: http://www.gadgetlite.com/2010/11/10/pharmajet-introduces-needle-free/

PINTO REIS, C. [*et.al.*] (2006). "Nanoencapsulation II. Biomedical applications and current status of peptide and protein nanoparticulate delivery systems." Nanomedicine : nanotechnology, biology, and medicine **2**(2): 53-65.

PONCELET, D. (2001). "Production of alginate beads by emulsification/internal gelation." Ann. New York Acad. Sci. **944**: 74-82.

PONCELET, D. [*et.al.*] (1992). "Production of alginate beads by emulsification/internal gelation. I. Methology." Appl. Microbiol. Biotechnol. **38**: 39-45.

QI R, [*et.al.*] (2004). "Effect of casein and protamine on the enzymatic degradation and the orally hypoglycemic action of insulin." Acta Pharma Sin **39**:844-848.

RAJAONARIVONY, M. [*et.al.*] (1993). "Development of a new drug carrier made from alginate." J. Pharm. Sci **82**: 912-917.

REIS, C. P. [*et.al.*] (2008). "Nanoparticulate biopolymers deliver insulin orally eliciting pharmacological response." Journal of Pharmaceutical Sciences **97**(12): 5290-5305.

RHODES, B. A. (1974). "Considerations in the radiolabeling of albumin." Seminars in nuclear medicine **4**(3): 281-293.

SAHA, G. B. (2004a). Radipharmaceutical and Methods of Radiolabeling. Fundamentals of Nuclear Pharmacy. G. B. SAHA. New York, USA, Springer**:** 79-110.

SAHA, G. B. (2004b). Instruments for Radiation Detection and Measurement. Fundamentals of Nuclear Pharmacy. G. B. SAHA. USA, Springer**:** 31-45.

SAHA, G. B. (2004c). Quality Control of Radiopharmaceutials. In: G. B. SAHA.Fundamentals of Nuclear Pharmacy. USA, Springer**.** 152-174.

SARMENTO, B. [*et.al.*] (2007b). "Oral Bioavailability of Insulin Contained in Polysaccharide NP." Biomacromolecules **8**(10): 3054-3060.

SARMENTO, B. [*et.al.*] (2007a). "Alginate/Chitosan NP are Effective for Oral Insulin Delivery." Pharmaceutical Research **24**(12): 2198-2206.

SCHECHTER, Y. [*et.al.*] (2005). "Albumin-insulin conjugate releasing insulin slowly under physiological conditions: a new concept for long-acting insulin." Bioconjug. Chem. **16**: 913-920.

SELAM, J. L. (2010). "Evolution of Diabetes Insulin Delivery Devices." Journal of Diabetes Science and Technology **4**(3): 505-513.

SHARP, P. F., GOATMAN, K. A. (2005). Nuclear Medicine Imaging. In: P. SHARP, Gemmell, H. G., Murray, A. D.Pratical Nuclear Medicine. UK, Springer**.** 1-20.

SHILPA, A., AGRAWAL, S. S., RAY, A. R. (2003). "Controlled delivery of drugs from alginate matrix." J. Macromol. Sci. **43**:187-221.

SILVA, C. M. [*et.al.*] (2006). "Insulin encapsulation in reinforced alginate microspheres prepared by internal gelation." Eur. J. Pharm. Sci. **29**:148-159.

SIMÕES, S. [*et.al.*] (2005). "Cationic hippodromes for gene delivery." Expert Opin. Drug Deliv. **2**:237-25.

SUBHASHINI, Y. (2013). "Insulin therapies: Current and future trends at dawn." World J Diabetes **4**(1):1-7.

TOUITOU, E., DONBROW, M., RUBINSTEIN, A. (1986). "Effective intestinal absorption of insulin in diabetic rats using new formulation approach." J. Pharm. Pharmacol. **32**:108-110.

URBANO, A. [*et.al.*] (2004). Microencapsulação de fármacos peptídicos em pectina pelo métodos emulsificação/gelificação interna: a albumina como fármaco modelo. Master, Universidade de Coimbra.

VANDENBERG, G. W., NOUÉ, J. D. L. (2001). "Evaluation of protein release from chitosan-alginate microcapsules produced using external or internal gelation." J. Microencapsul. **18**: 433-441.

WANG, Y. Chen [*et.al.*] (2011). "Technetium-99m-Labeled Autologous Serum Albumin: A Personal-Exclusive Source of Serum Component." Journal of Biomedicine and Biotechnology **2011**.

WANG, L. CHAN. [*et.al.*] (1997). "Effect of cellulose derivatives on alginate microspheres prepared by emulsification." J. Microencapsul. **14**: 545-555.

WANG, Y. CHIEN (1996). "Human Insulin: Basic Sciences to Therapeutic Uses." Drug Development and Industrial Pharmacy **22**(8): 753-789.

WANG, Y.F. [*et.al.*] (2007). "On-Site Preparation of Technetium-99m Labeled Human Serum Albumin for Clinical Application." The Tohoku Journal of Experimental Medicine **211**(4): 379-385.

WILCZEWSKA, A. Z., NIEMIROWICZ, K., MARKIEWICZ, K. H., CAR, H. (2012). "NP as drug delivery systems." Pharmacological Reports **64**: 1020-1037.

WILD, S. [*et.al.*] (2004). "Global Prevalence of Diabetes: Estimates for the year 2000 and projections for 2030." Diabetes Care **27**(5): 1047-1053.

WILLIAMS, M. J. AND T. DEEGAN (1971). "The process inovolved in the binding of technetium-99m to human serum albumin." The International Journal of Applied Radiation and Isotopes **22**(12): 767-774.

WOITISKI, C. B. [*et.al.*] (2009a). Colloidal carrier integrating biomaterials for oral insulin delivery: Influence of component formulation on physicochemical and biological parameters.

WOITISKI, C. B. [*et.al.*] (2009b). "Design for optimization of NP integrating biomaterials for orally dosed insulin." European Journal of Pharmaceutics and Biopharmaceutics **73**(1): 25-33.

YOKOYAMA, A. [*et.al.*] (1975). "The role of ascorbic acid with the ferric ion in labelling human serum albumin with99 mTc." Int J Appl Radiat Isot **26**(5): 291-299.

ZOLLE, I. (2007). Technetium-99m Pharmaceuticals. Preparation and Quality Control in Nuclear Medicine. I. ZOLLE. Austria, Springer.

ZOLLE, I. [*et.al.*] (1973). "Contribution to the study of the mechanism of labelling human serum albumin (HSA) with technetium-99m." The International Journal of Applied Radiation and Isotopes **24**(11): 621-626.

# 7. Annex

## I – Results of $^{99m}$Tc-BSA biodistribution in % of administered activity/mg

| | 0 min (mean±SD) | 30 min (mean±SD) | 60 min (mean±SD) | 90 min (mean±SD) | 120 min (mean±SD) | 180 min (mean±SD) | 360 min (mean±SD) | 1440 min (mean±SD) |
|---|---|---|---|---|---|---|---|---|
| Stomach's epithelium | 0.0029 ±0.0002 | 0.0059 ±0.0004 | 0.0245 ±0.0024 | 0.0256 ±0.0016 | 0.0347 ±0.0033 | 0.0082 ±0.0004 | 0.0046 ±0.0003 | 0.0000 ±0.0000 |
| Stomach's content | 0.5077 ±0.0109 | 0.4452 ±0.0316 | 0.3959 ±0.0859 | 0.2691 ±0.0579 | 0.1175 ±0.0308 | 0.0427 ±0.0232 | 0.0091 ±0.0064 | 0.0000 ±0.0000 |
| Duodenum's epithelium | 0.0000 ±0.0000 | 0.0014 ±0.0003 | 0.0024 ±0.0002 | 0.0031 ±0.0008 | 0.0032 ±0.0006 | 0.0030 ±0.0006 | 0.0000 ±0.0000 | 0.0000 ±0.0000 |
| Duodenum's content | 0.0000 ±0.0000 | 0.1149 (±0.0241 | 0.0098 (±0.0023 | 0.0142 (±0.0011 | 0.0044 (±0.0018 | 0.0021 ±0.0007 | 0.0004 ±0.0002 | 0.0000 ±0.0000 |
| Small intestine´s epithelium | 0.0000 ±0.0000 | 0.0003 ±0.0001 | 0.0017 ±0.0004 | 0.0019 ±0.0003 | 0.0022 ±0.0005 | 0.0021 ±0.0004 | 0.0000 ±0.0000 | 0.0000 ±0.0000 |
| Small intestine's content | 0.0000 ±0.0000 | 0.1686 ±0.0396 | 0.2335 ±0.0322 | 0.2436 ±0.0268 | 0.0387 ±0.0051 | 0.0301 ±0.0057 | 0.0022 ±0.0008 | 0.0000 ±0.0000 |
| Large intestine's epithelium | 0.0000 ±0.0000 | 0.0000 ±0.0000 | 0.0000 ±0.0000 | 0.0030 ±0.0009 | 0.0064 ±0.0010 | 0.0043 ±0.0006 | 0.0000 ±0.0000 | 0.0000 ±0.0000 |
| Large intestine's content | 0.0000 ±0.0000 | 0.0000 ±0.0000 | 0.0000 ±0.0000 | 0.1047 ±0.0192 | 0.1309 ±0.0275 | 0.1624 ±0.0465 | 0.0128 ±0.0020 | 0.0000 ±0.0000 |
| Liver | 0.0000 ±0.0000 | 0.0001 ±0.0001 | 0.0002 ±0.0001 | 0.0002 ±0.0000 | 0.0002 ±0.0000 | 0.0002 ±0.0001 | 0.0000 ±0.0000 | 0.0000 ±0.0000 |
| Lung | 0.0000 ±0.0000 | 0.0000 ±0.0000 | 0.0000 ±0.0000 | 0.0000 ±0.0000 | 0.0000 ±0.0000 | 0.0000 ±0.0000 | 0.0000 ±0.0000 | 0.0000 ±0.0000 |
| Tyroid | 0.0000 ±0.0000 | 0.0000 ±0.0000 | 0.0000 ±0.0000 | 0.0000 ±0.0000 | 0.0000 ±0.0000 | 0.0000 ±0.0000 | 0.0000 ±0.0000 | 0.0000 ±0.0000 |
| Muscle | 0.0000 ±0.0000 | 0.0000 ±0.0000 | 0.0000 ±0.0000 | 0.0000 ±0.0000 | 0.0000 ±0.0000 | 0.0000 ±0.0000 | 0.0000 ±0.0000 | 0.0000 ±0.0000 |
| Blood | 0.0000 ±0.0000 | 0.0000 ±0.0000 | 0.0000 ±0.0000 | 0.0000 ±0.0000 | 0.0000 ±0.0000 | 0.0000 ±0.0000 | 0.0000 ±0.0000 | 0.0000 ±0.0000 |
| Kidneys | 0.0000 ±0.0000 | 0.0000 ±0.0000 | 0.0000 ±0.0000 | 0.0002 ±0.0001 | 0.0002 ±0.0000 | 0.0000 ±0.0000 | 0.0000 ±0.0000 | 0.0000 ±0.0000 |

## II – Results of $^{99m}$Tc-BSA-NP biodistribution in % of administered activity/mg

| | 0 min (mean±SD) | 30 min (mean±SD) | 60 min (mean±SD) | 90 min (mean±SD) | 120 min (mean±SD) | 180 min (mean±SD) | 360 min (mean±SD) | 1440 min (mean±SD) |
|---|---|---|---|---|---|---|---|---|
| Stomach's epitelium | 0.0262 (±0.0009 | 0.0273 ±0.0024 | 0.0309 ±0.0079 | 0.0367 ±0.0071 | 0.0029 ±0.0007 | 0.0020 ±0.0003 | 0.0017 ±0.0006 | 0.0000 ±0.0000 |
| Stomach's content | 0.4989 ±0.0323 | 0.3898 ±0.0320 | 0.2705 ±0.0340 | 0.2090 ±0.0542 | 0.1407 ±0.0337 | 0.0395 ±0.0126 | 0.0084 ±0.0008 | 0.0000 ±0.0000 |
| Duodenum's epitelium | 0.0000 ±0.0000 | 0.0019 ±0.0005 | 0.0033 ±0.0003 | 0.0021 ±0.0006 | 0.0006 ±0.0001 | 0.0004 ±0.0001 | 0.0000 ±0.0000 | 0.0000 ±0.0000 |
| Duodenum's content | 0.0000 ±0.0000 | 0.0939 ±0.0170 | 0.0462 ±0.0075 | 0.0124 ±0.0028 | 0.0028 ±0.0006 | 0.0026 ±0.0005 | 0.0020 ±0.0003 | 0.0000 ±0.0000 |
| Small intestine´s epitelium | 0.0000 ±0.0000 | 0.0006 ±0.0000 | 0.0006 ±0.0001 | 0.0021 ±0.0002 | 0.0005 ±0.0001 | 0.0002 ±0.0001 | 0.0000 ±0.0000 | 0.0000 ±0.0000 |
| Small intestine's content | 0.0000 ±0.0000 | 0.1550 ±0.0236 | 0.1987 ±0.0298 | 0.0803 ±0.0105 | 0.0249 ±0.0044 | 0.0214 ±0.0015 | 0.0015 ±0.0003 | 0.0000 ±0.0000 |
| Large intestine's epitelium | 0.0000 ±0.0000 | 0.0000 ±0.0000 | 0.0000 ±0.0000 | 0.0028 ±0.0005 | 0.0067 ±0.0005 | 0.0018 ±0.0005 | 0.0000 ±0.0000 | 0.0000 ±0.0000 |
| Large intestine's content | 0.0000 ±0.0000 | 0.0000 ±0.0000 | 0.0000 ±0.0000 | 0.1523 ±0.0351 | 0.2590 ±0.0359 | 0.1486 ±0.0343 | 0.0626 ±0.0059 | 0.0000 ±0.0000 |
| Liver | 0.0000 ±0.0000 | 0.0000 ±0.0000 | 0.0000 ±0.0000 | 0.0000 ±0.0000 | 0.0002 ±0.0001 | 0.0002 ±0.0001 | 0.0000 ±0.0000 | 0.0000 ±0.0000 |
| Lung | 0.0000 ±0.0000 | 0.0000 ±0.0000 | 0.0000 ±0.0000 | 0.0000 ±0.0000 | 0.0000 ±0.0000 | 0.0000 ±0.0000 | 0.0000 ±0.0000 | 0.0000 ±0.0000 |
| Tyroid | 0.0000 ±0.0000 | 0.0000 ±0.0000 | 0.0000 ±0.0000 | 0.0000 ±0.0000 | 0.0000 ±0.0000 | 0.0000 ±0.0000 | 0.0000 ±0.0000 | 0.0000 ±0.0000 |
| Muscle | 0.0000 ±0.0000 | 0.0000 ±0.0000 | 0.0000 ±0.0000 | 0.0000 ±0.0000 | 0.0000 ±0.0000 | 0.0000 ±0.0000 | 0.0000 ±0.0000 | 0.0000 ±0.0000 |
| Blood | 0.0000 ±0.0000 | 0.0000 ±0.0000 | 0.0000 ±0.0000 | 0.0000 ±0.0000 | 0.0000 ±0.0000 | 0.0000 ±0.0000 | 0.0000 ±0.0000 | 0.0000 ±0.0000 |
| Kidneys | 0.0000 ±0.0000 | 0.0000 ±0.0000 | 0.0000 ±0.0000 | 0.0000 ±0.0000 | 0.0000 ±0.0000 | 0.0000 ±0.0000 | 0.0000 ±0.0000 | 0.0000 ±0.0000 |